# AIRBORNE MULTISPECTRAL IMAGERY FOR CLASSIFICATION OF INTERTIDAL HABITAT, FRASER RIVER, BRITISH COLUMBIA

by

JENNIFER ANTHEA AITKEN

B. A., Geography, The University of Texas, 1990

A THESIS SUBMITTED IN PARTIAL FULFILLMENT OF THE

REQUIREMENTS FOR THE DEGREE OF MASTER OF SCIENCE

in

THE FACULTY OF GRADUATE STUDIES

Department of Oceanography

We accept this thesis as conforming to the required standard

THE UNIVERSITY OF BRITISH COLUMBIA

December 1994

In presenting this thesis in partial fulfilment of the requirements for an advanced degree at the University of British Columbia, I agree that the Library shall make it freely available for reference and study. I further agree that permission for extensive copying of this thesis for scholarly purposes may be granted by the head of my department or by his or her representatives. It is understood that copying or publication of this thesis for financial gain shall not be allowed without my written permission.

Department of _Oceanography_

The University of British Columbia
Vancouver, Canada

Date _Dec. 22, 1994_

# ABSTRACT

In intertidal environments, complex vegetation associations, hydrodynamics, and substrate variabilities make accurate mapping and monitoring difficult. Airborne multispectral imaging systems offer a synoptic view with the advantage of programmable bandset selection in the visible and near infrared (NIR), increased spatial resolution compared to satellite imaging systems and greater spectral resolution compared with aerial photographs. Eight flight lines of image data of an island marsh complex in the Main Arm of the Fraser River, British Columbia were collected on June 19, 1992 with a Compact Airborne Spectrographic Imager (CASI). An eleven channel bandset was configured in the visible and NIR with a spatial resolution (pixel size) of 3.5 $m^2$.

Spectral signatures of dominant vegetation communities (forest, willow, cattail, sedge, bulrush) and tidal flat, drift logs and necrotic biomass were generated from the image and used in a supervised classification to produce a habitat map. Close coexistence and similar spectral response complicated differentiation of sedge and cattail. Vertical growth of bulrush increased contribution of soil background and affected spectral response. The vegetation index (NIR-red/NIR+red) was found to be insufficient in estimating green biomass in areas containing a high percentage of necrotic biomass or silt covered vegetation.

Results of the classification are presented in an error matrix. Vegetation communities and substrate classify 70%-82% correct, individual training areas 61% to 89% correct. Lower accuracies were found in mixed sedge communities (70%) and the dead biomass class (74%). Nonvegetated areas (tidal flat and drift logs) exhibit the most distinct spectral response, 81% and 82% correct.

Two surveys of the marsh were conducted on foot in Ladner Marsh in spring and summer to field test the classified map. Fourteen sites were visited, of which three indicated some degree of misclassification, providing a field test accuracy of 78%.

Spatial accuracy is determined by an overlay of GPS-referenced ground truth with the classified map. Spatial agreement between cattail, sedge and bulrush ground truth was 20.4 m., 14.4 m., and 53.5 m. respectively. Sedge had the greatest number of classified pixels and bulrush the least, suggesting the influence of population size in the agreement. Poor geometric rectification of imagery degraded agreement.

# TABLE OF CONTENTS

# LIST OF TABLES

# LIST OF FIGURES

## LIST OF FIGURES (CON'T)

Figure                                                              page

# ACKNOWLEDGMENTS

# I. INTRODUCTION

The Fraser River of British Columbia is one of the richest salmon streams in the world and supports a multitude of bird species in the path of the Pacific flyway. From its headwaters in the northern Rocky Mountains of British Columbia the Fraser River flows to the Strait of Georgia. Where the river water mixes with the saline tidal waters of the Pacific there exists the Fraser River delta, of which 2813 hectares is estuarine marsh (Ward et al. 1992). Urban, industrial, and residential development in the Fraser River delta began 150 years ago and is expected to continue in the future. To best manage the Fraser River's natural estuarine resources, fish and wildlife agencies require an accurate and up to date inventory of key wildlife and fisheries habitat. Large, difficult to access areas of marsh must be mapped in detail (approximately 1:5,000 scale), and frequently updated via a precise and efficient monitoring method.

Wetlands are difficult areas to map using remotely sensed data due to hetereogeneity in the environment. Soil background, leaf orientation and canopy structure can be as important as the optical properties of the wetland vegetation (Bartlett and Klemas 1981, Ernst-Dottavio et al. 1981). Dead biomass from previous years growth collects in the vegetation canopy and affects the spectral response of living vegetation. (Tucker 1979). Phenotypic differences and a highly intermixed growing environment limit species discrimination. Ground truth and familiarity with plant ecology are requisite to image interpretation and confusion over boundary delineations are reflections of the reality of wetlands (Howland 1980). By the same token,

1

inferences about tidal range, drainage, and elevation can be made with knowledge of the growing habits of these species (Moody 1978, Best et al. 1981).

Traditionally, mapping and monitoring of wetlands has relied on aerial photography and color and color infrared (CIR) film (Anderson and Roos 1991). Air photos have the most superior spatial resolution of current remote sensing systems, but the spectral resolution (bandwidth) is limited to the type and number of spectral filters used on the film, and the airphoto must be digitized for computer analysis. Filter bandwidths can be hundreds of nanometers wide and researchers often succeed only in delineating general areas, such as "marsh" or "wet meadow" (Anderson and Roos 1991, Howland 1980, Brown 1978).

Satellite imagery has been used in wetland mapping, but the low spatial resolution (30 meters for Landsat's Thematic Mapper) hinders delineation of communities. Bartlett and Klemas (1981) report separation of low marsh (salt marsh cordgrass) and high marsh (salt meadow grass and spike grass) was poor at peak growth times, and separable only in early winter. Ernst-Dottavio et al. (1981), using Landsat imagery of Indiana, report cattail and rush zones were separable but the sedge/forb zone and shrub swamp (willow) were difficult to discriminate. In areas of partial vegetation cover (30-60%), the classes were easily mixed, attributed to the influence of the unvegetated background. Satellite data are often used in conjunction with airborne data for an integrated regional approach to identifying wetlands (Gilmer et al. 1980, Jensen et al. 1986, and Butera 1983).

Airborne digital imaging instruments such as the Compact Airborne Spectrographic Imager (CASI) can achieve spatial resolutions of one or more meters in the 400 to 900 nm spectral range, recording data in digital format (Borstad and Hill 1989, Anger et al. 1990). The spectral resolution (bandwidth) of these instruments instrument is in the range of 2 to 50 nm, and the width and placement of bands is set by the user. (See Appendix B). The increased spectral sensitivity allows more detailed classification of wetlands than is possible from aerial photographs or satellite-borne imaging instruments (Jensen et al. 1986). Butera (1983) used airborne imagery of 7.6 meter spatial resolution to discriminate *Spartina spp.* (cordgrass), *Distichlis spp.* (spike grass), and *Juncus spp.* (soft rush) communities from *Typha spp.* (cattail) communities with an accuracy of 82% when compared with ground truth. Butera reports these communities are nondistinctive in Landsat imagery. Christensen et al. (1989) employed airborne multispectral data (5.6 meter spatial resolution) to measure changes in an estuarine wetland of the Savannah River over a four year period at an accuracy level of 85 to 88%. The categories consisted of persistent emergent vegetation, nonpersistent emergent vegetation , scrub/shrub, and swamp forest. Jensen et al. (1986) used the same categories, adding algal mats to the classification, and reported airborne MSS accurate to 83% for vegetation discrimination and detection of recent patterns in vegetation growth. Savastano et al. (1984) mapped emergent vegetation in Florida and found the near infrared to contain the most information, and the blue visible to contain the least, due to a poor signal to noise ratio. Geometric distortions in the image data were found to degrade spatial accuracy, and sun glint on the water distorted the radiometric response.

Several authors have used remote sensing for green biomass estimations from a ratio of infrared to visible red spectral response, including Tucker (1979), Bartlett and Klemas (1981), Christensen et al. (1989) and Penuelas et al. (1993). The impetus is to define a method of estimating biomass, but the influence of underlying necrotic biomass can reduce the NIR response of green vegetation, making the ratio an unreliable indicator of the proportion of living biomass (Drake 1976, Bartlett and Klemas 1981).

The purpose of this thesis is to evaluate the use of airborne multispectral imagery for the production of a classified map of specific vegetation communities identified by dominant indicator species. Eight flight lines of image data from a Compact Airborne Spectrographic Imager (CASI), were collected June 19, 1992, by Borstad Associates of Sidney, British Columbia as part of an Environmental Innovations Program (EIP) sponsored by Environment Canada. Five flight lines covering the eastern half of the South Arm Estuary were combined into an image mosaic. Ground truthing in Ladner Marsh identified the main vegetation communities and areas significant to marsh productivity (tidal flats and accumulations of drift logs and necrotic biomass). The vegetation communities and surrounding areas were located in the imagery and spectral signatures were determined for floodplain forest, willow, cattail, sedge and bulrush communities, as well as tidal flat, necrotic biomass, and drift logs. A maximum likelihood classification was performed and the performance of each spectral signature is presented in a confusion matrix. Field tests were conducted with the classified map to test classification accuracy. Spatial accuracy of the classified map is estimated by comparison with GPS-referenced ground truth samples. A near infrared to visible red ratio was calculated to estimate vegetation biomass and to determine the influence

of underlying necrotic biomass on the spectral response of a green vegetation canopy.

## 2. THE SOUTH ARM ESTUARY

## 2.1 Historical Development

The South Arm Marshes Wildlife Management Area, referred to here as the South Arm Estuary, consists of the stable Ladner Marsh and a somewhat transient island group made up of Rose, Kirkland, Gunn, Barber and Duck Islands in the south arm of the Fraser River near the confluence with the Strait of Georgia (Figure 1). The area is bounded by Woodward Reach to the north, Sea Reach to the west and south, and River Road on the far side of Ladner Marsh to the east. The South Arm Estuary is generally classified as brackish marsh and floodplain forest (Ward 1992). Residential development is currently taking place adjacent of Ladner Marsh, on the east side of Ferry Road. Although the general outline of the marsh has not changed in 50 years (Bradfield and Porter 1982), considerable changes have occurred in the last 150 years (Tamburi and Hays 1978). In Figure 2, hydrographic data from 1827 shows the main distributary channel of the south arm to be the South Channel (present day Canoe Pass in Fig. 1), with one main island located in the middle of the channel. By 1860, this sand island had broken up into several smaller islands which are present today as the South Arm Estuary (Figure 3). In 1922, Woodward Reach was dredged and developed as the main navigation channel, and Ladner Reach, Sea Reach and Canoe Pass lost 86% of the river flow and the present configuration was reached (Tamburi and Hays 1978).
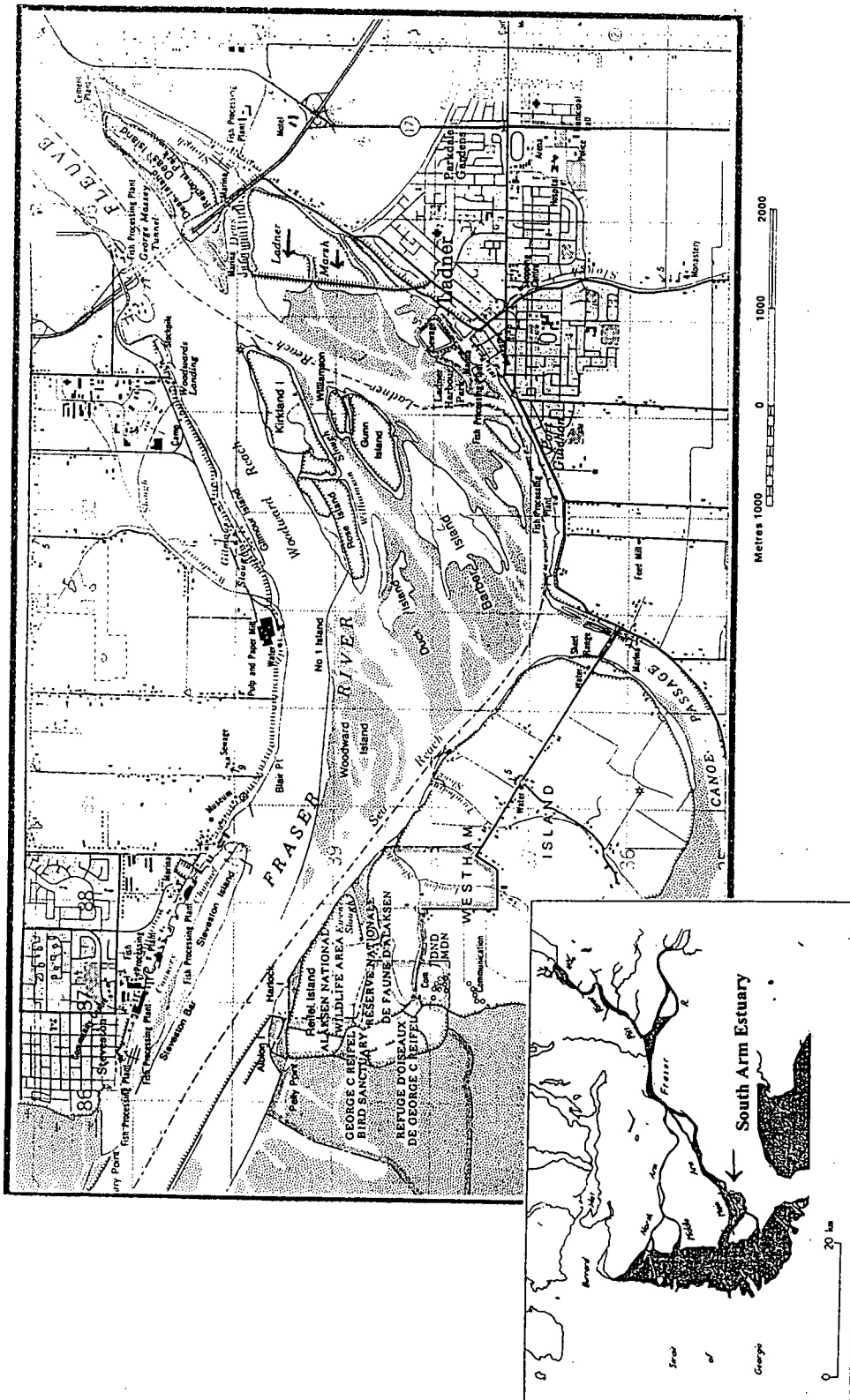
**Figure 1.** Map showing the South Arm Estuary, Fraser River, British Columbia. The South Arm Estuary includes Ladner Marsh, Kirkland, Rose, Duck, Gunn, and Barber Islands.

7
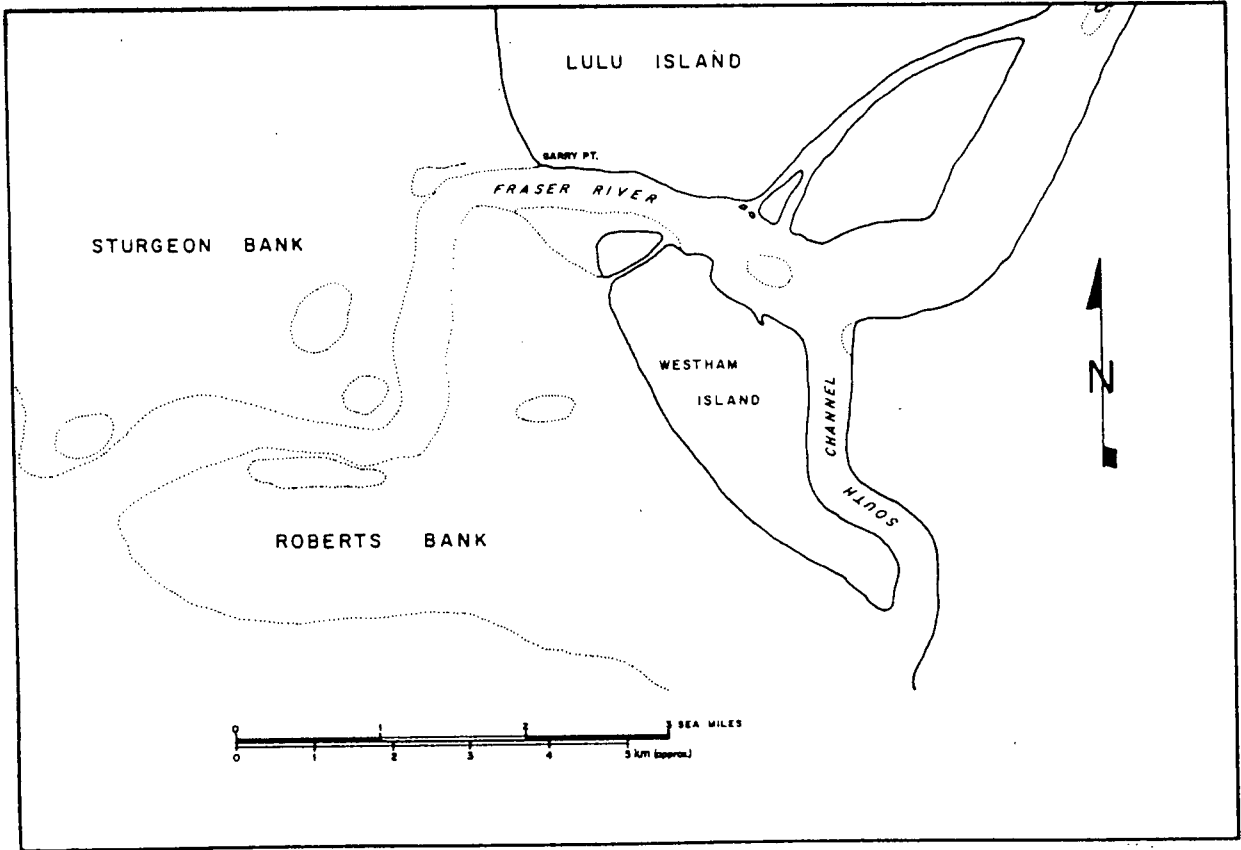
**Figure 2.** Map of the Fraser River foreshore, 1827, prior to the natural development of the South Arm Estuary. (Adapted from Tamburi and Hays 1978).
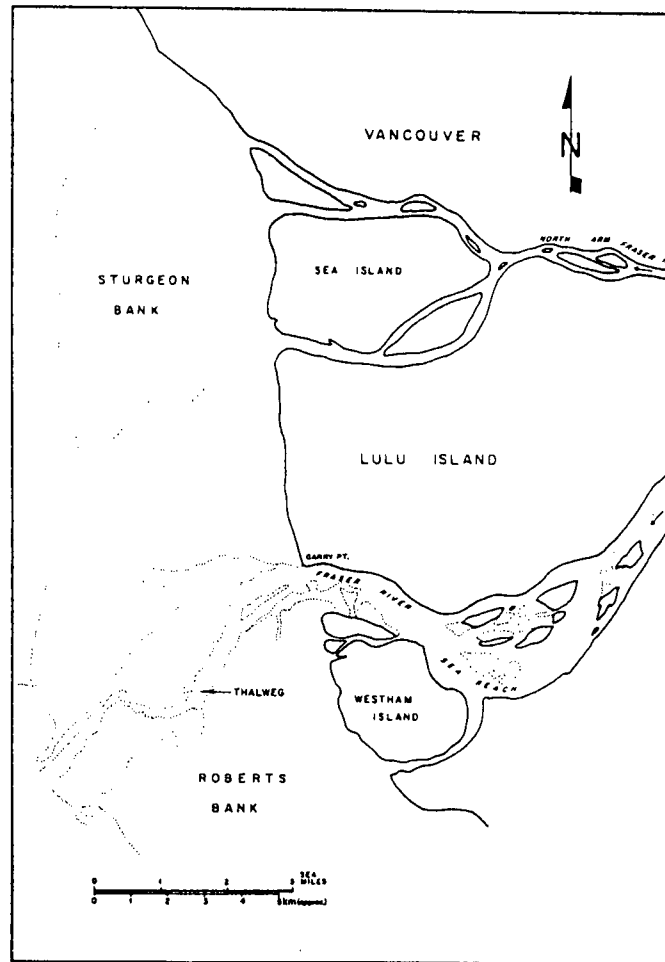
**Figure 3.** Map of the Fraser River foreshore, 1860, when Sea Reach was still the main navigation channel. Woodward Reach was developed as the main navigation channel in 1922. (Adapted from Tamburi and Hays 1978).

## 2.2. Physical Environment

Tides in the estuary are highest and lowest in winter (December through February) due to decreased flow from the Fraser River. At a low flow of 340 m$^3$/s, the salt wedge from the Strait of Georgia is upstream of Deas Island. The winter position is at Deas Island on the eastern boundary of the South Arm Estuary. At freshet, when the average flow of the Fraser is 9,600 m$^3$/s, the salt wedge is at Sand Heads, seaward of the Estuary. Tamburi and Hays (1978) report each smaller channel has a mini salt wedge configuration. Dyking, done in the last century and early in this century, ends tidal inundation and changes plant composition to more terrestrial species. This is particularly evident on Kirkland and Rose Island, where agricultural lands are maintained (Moody 1974).

The vegetation in this salinity transition zone is widely believed to be linked to tidal range and drainage. (Hunter 1983, Bradfield and Porter 1982, Moody 1974, and Forbes 1972). Hoos and Packman (1974) note that in an area of turbid water where phytoplankton production is low, such as in this estuary, the marsh vegetation assumes importance as a primary producer. Ladner Marsh, part of the main delta land mass, is an older and more stable environment than the islands, and over 50 species of vegetation have been identified there (Bradfield and Porter 1982). The dominant species of Ladner Marsh are black cottonwood (*Populus* spp.), willow (*Salix* spp.), cattail (*Typha* spp.), sedge (*Carex* spp.) and bulrush (*Scirpus* spp.) which continue to dominate seaward in the South Arm Estuary as the more diverse species lessen in occurrence. Species diversity decreases seaward due to increased tidal inundation and salinity, and the transitional nature of the substrate (Kistritz

1990). Plants contribute to sediment accretion and probably can be accredited with much of seaward south arm marsh development (Moody 1978). Intertidal mud flats of fine-grained soils are common, particularly where channels bend and water velocity slows. The supersaturated mud support algae and vascular aquatics. Organic decomposition is just below the soil surface.

# 3. HABITAT CLASSIFICATION SCHEME

The habitat classes are listed below. Vegetation communities are identified by a dominant species determined from field sampling and the literature. Common categories for wetland mapping include forest, cattail, sedge, and rush. These categories are found in the National Wetland Inventory of the U.S. Fish and Wildlife Service and the Fraser River Estuary Management Program (FREMP) of the Department of Fisheries and Oceans, British Columbia (Jensen et al. 1986, Kistritz 1989).

## 3.1 Vegetation Communities

### 3.1.1. Floodplain forest

Floodplain forest is found on stable, well-drained substrate, above tidal influences and provides an excellent habitat for birds (Forbes 1972, Bradfield and Porter 1982). The most dominant tree species in the South Arm Estuary is *Populus trichocarpa* (black cottonwood), associated with red alder (*Alnus rubra*), dogwood *(Cornus stolonifera)* and blackberry (*Rubus ursinus*). A significant amount of woodland exists in Ladner Marsh and occurs with decreasing frequency seaward. The trees often have an understory of shrubs and grasses, which include willow and blackberry bushes.

### 3.1.2. Willow

Willow (*Salix spp.*) grows as a bush to 4-8 meters in height. The leaves are 2-10 cm wide, dark green, smooth, and somewhat shiny. Willow is found along larger drainage channels, levees, and other areas which are likely to be flooded only at the highest of winter storm tides (Bradfield and Porter

1982). The roots are thought to stabilize sediments and build a substrate for other species (Weinmann and Boule 1984). Willow was sampled during ground truthing in dense configurations at higher elevations in Ladner Marsh, and along the waterline growing in conjunction with many species, among which none were dominant. In very wet areas, willow is associated with cattail, purple loosestrife (*Lythrum salicaria*) and beach grass *(Festuca arundinacea)* (Weinmann and Boule 1984).

### 3.1.3. Cattail

Cattail, or *Typha spp.*, grows 1-2 meters in height in fresh to brackish water. The main stem of the female flower is topped by the characteristic brown cylinder. Narrow dark green leaves grow up to the same height as the main stem. Most cattail grows at a slightly higher elevation than bulrush or sedge, and can occur farther away from water, although all three species can be found together (Weinmann and Boule 1984, Forbes 1972). Cattail often grows in circular stands, which indicates species expansion from a single pioneer cattail. Often found at shorelines, cattail stands are thought to promote siltation (Howland 1980). Dead cattail can persist through the winter, and if hydrologic flushing is insufficient, can accumulate as stands of dead biomass (Mark Adams, pers. comm. 1994). Forbes (1972) reported cattail very common on Reifel and Westham Islands. Cattail grows with several different species, among them purple loosestrife (*Lythrum salicaria*), dock (*Rumex spp.*), beach grass (*Festuca arundinacea*), Douglas spiraea (*Spiraea douglasii*) , arrowhead or wapato (*Sagittaria spp.*), soft rush (*Juncus spp.*) , reed canarygrass (*Phalaris arundinacea*), and willow (*Salix spp.*) (Weinmann and Boule 1984).

13

### 3.1.4 Sedge

Sedge, or *Carex spp.*, is prominent in brackish coastal marshes from northern California to southern Alaska and occurs frequently in the estuary. Bradfield and Porter (1982) report sedge to have the greatest biomass of any species in Ladner Marsh, and Moody (1978) reports sedge to have the highest growth rate of all wetland plants studied. Sedge grows up to 1 meter in height as a cluster of slender, light green leaves, 2-6 mm wide and 30 cm long (Weinmann and Boule 1984). Peak growth rate is in July (Moody 1978), approximately two weeks after image collection for this study. Marshland sedge prefers regularly flooded and drained areas and is found along tidal creeks. Sedge grows indiscriminately with many other species including bulrush (*Scirpus spp.*), soft rush (*Juncus spp.*), dock (*Rumex spp.*), *Agrostis spp*, beach grass (*Festuca arundinacea*), seaside arrowgrass (*Triglochin maritimum*), arrowhead (*Sagittaria spp.*), and cattail. McLaren (1972) and Weinmann and Boule (1984) report smaller bulrush species are often mistaken for sedge, and sedge could be over represented, particularly on Duck, Barber and Woodward Islands. Ground truthing located dense populations of sedge lining tidal channels between Duck and Barber Islands.

### 3.1.5. Bulrush

Bulrush, or *Scirpus spp.*, averages 2 meters in height with a stem diameter of up to 3 cm. The color is gray-green, and brown spikelets appear at the top of the stem. During ground truthing, bulrush was found in saturated mud at the lowest elevations, adjacent to tidal flats and channels. At high tide bulrush is almost completely submerged. Bulrush grows with increasing frequency seaward, often in linear swaths at or above the low tide line, and was observed to be almost completely submerged at high tide. Bulrush is

described as a primary colonizer of tidal flats (Forbes 1972, Moody 1978). Sedge, spike grass (*Distichlis spp.*), and soft rush (*Juncus spp.*) are associated with bulrush and often grow as an understory, particularly in Ladner Marsh, also noted by Forbes (1972). Other species observed with bulrush include arrowhead (*Sagittaria spp.*), beach grass (*Festuca arundinacea*), and less occasionally, cattail (Bradfield and Porter 1982).

## 3.2. Tidal flats

Tidal flats support a high population of invertebrates (zooplankton, phytoplankton, crabs, shrimp and oysters) and benthic vegetation, including several species of blue-green algae (Hoos and Packman 1974). The soil is likely to be highly saturated (up to 100%). At low tide the flats are exposed, along with algal mats, intertidal debris, small potholes of water approximately 10-20 cm diameter, and petroleum residues. The soil can be highly organic.

## 3.3. Drift logs

Significant numbers of stray logs collect in the estuary, particularly large logs of cedar and fir which escape from log booms in the river. The logs are deposited inland during storms or at very high tides and can become permanent fixtures of the marsh. Other logs are temporarily left in lowland areas. Accumulations of drift logs influence drainage patterns, sediment deposition, and nutrient cycles.

## 3.4. Dead biomass

Areas of the marsh incompletely flushed by the river or the tide are identified by accumulations of necrotic vegetation from previous seasons. Cattail is particularly resistant to decay. Bulrush is less persistent, although parts of some stalks were found in winter and early spring. Sedge dies away completely above the surface in winter and is not part of this category. Stands of dead biomass are easily located in winter and early spring, but can be obscured by living vegetation in the summer. Like drift logs, dead biomass influences nutrient cycles and gives clues to the flushing regime of the marsh.

## 4. DATA COLLECTION

### 4.1. Flight Parameters and Instrument Bandset

Eight flight lines of CASI imagery were collected on June 19, 1992 at midday and very low tide. Seasonally, this is the time of peak vegetation growth (Moody 1978). The bandset and flight parameters are listed in Table 1. Of eight flight lines collected, five flight lines (2 through 6) covering the eastern portion of the South Arm Estuary were combined into an image mosaic. Figure 4 shows the mosaic of flight lines 2-6, simulating a true color image by displaying Band 6 (658-670 nm), Band 3 (545-556 nm), and Band 1 (450-503 nm) as red, green, and blue, respectively. Given the aircraft altitude of 2896 m (9500 ft.), a ground speed of 47 m/s and an instrument integration time of 75 milliseconds the spatial resolution (pixel size) of the imagery is 3.5 meters.

Radiance measurements collected in each flight line are a function of the surface viewed by the instrument and the following factors: variations in incoming solar radiation, instrument calibration error and drift, instrument radiometric resolution, signal digitization errors, and effects of the intervening atmosphere (including attenuation and path radiance). Variations in incoming solar radiation caused by differences in sun angle are best avoided during data collection, by flying all flight lines in the same direction either towards or away from the sun. In this project flight lines were flown in both the north and south direction. In Figure 4, the effects of varying sun angle are seen as differences of tone on the water's surface.

**Table 1.** CASI image bandset, South Arm Estuary, June 19, 1992.

| Band # | Wavelength (nm) | Bandwidth (nm) | Spectral region |
|--------|-----------------|----------------|-----------------|
| 1 | 450-503 | 53 | Clear water penetration |
| 2 | 510-529 | 19 | Vegetation pigment absorption |
| 3 | 545-556 | 11 | Chlorophyll reflectance peak |
| 4 | 564-604 | 10 | Chlorophyll absorption |
| 5 | 632-643 | 11 | Chlorophyll absorption |
| 6 | 658-670 | 12 | Chlorophyll absorption |
| 7 | 671-686 | 15 | Chlorophyll absorption |
| 8 | 687-698 | 11 | Reduced reflectance for dead vegetation |
| 9 | 699-714 | 15 | Red edge of plant reflectance |
| 10 | 748-754 | 6 | Live/dead vegetation discrimination, substrate identification |
| 11 | 861-879 | 9 | Live/dead vegetation discrimination, substrate identification |

| | |
|---|---|
| Aircraft altitude | 9500 ft., 2896 m. |
| Ground speed | 105 mph, 47 m/sec. |
| Integration time | 75 millisec. |
| Swath width | 1.7 km; 30% overlap |

*Sources: Gates et al. (1965), Hoffer (1978), Lillesand and Kiefer (1987), Zacharias et al. (1992).*

18
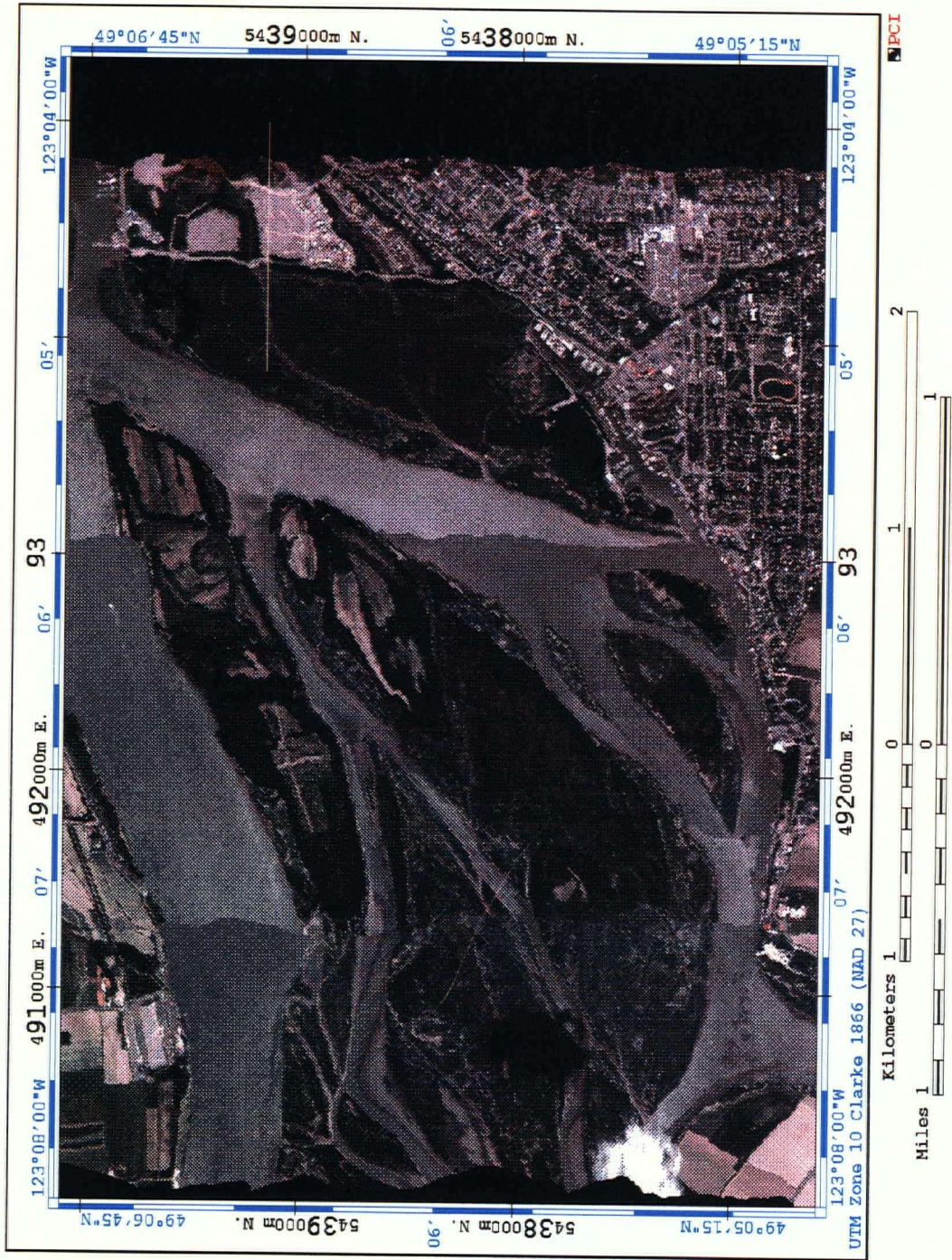
Fig. 4. Image mosaic of the South Arm Estuary, June 1992. Displayed bands are 6 (658-670 nm), 3 (545-556 nm), and 1 (450-503 nm).

19

The marsh vegetation reflectance was less affected by the changes in sun angle because atmospheric scattering of incoming solar radiation primarily affects the shorter wavelengths of the blue visible region whereas vegetation is best detected in the green, visible red, and near infrared region of the electromagnetic spectrum (Slater 1989). However, flight line 6 (seen in the far left of the mosaic in Figure 4) presented difficulties in spectrally separating cattail and sedge grass because of an overall lack of contrast in the radiance values in flight line 6. It is possible to radiometrically match different flight lines by adding or subtracting a constant value from one or all channels in a flight line. This approach can not work if the pixel by pixel contrast is diminished by too much or too little incoming solar radiation. Adding or subtracting a constant value will not recover a loss of contrast in an image. Therefore, because of the poor contrast, flight line six was eliminated from the classification.

Radiance measurements were collected in eleven spectral bands in the 450 to 870 nm range of the electromagnetic spectrum. This bandset was originally designed for water penetration and water quality estimation; bands located in the blue, green, red and NIR region allow for vegetation discrimination (Lillesand and Kiefer 1987). There is no standard bandset for intertidal vegetation, due mainly to variations in the environment and the atmosphere, as well as the infancy of airborne remote sensing. Band 1 (450-503 nm), located in the blue visible region, is relatively wide (53 nm) to increase the signal to noise ratio for the shorter wavelengths. Ten narrower bands (10-19 nm bandwidth) are located in the green, red, and near infrared (NIR) regions where vegetation pigments exhibit characteristic absorptions and reflections of electromagnetic energy. The instrument detectors were found to

be saturated in Band 11 (861-870 nm) and this channel was excluded from analysis.

## 4.2. Image Geocorrection and Registration

Spatial accuracy of remotely sensed imagery depends on registration of the image in space and time to a reference projection. Imagery is initially corrected to remove aircraft motion using measurements of aircraft roll and pitch recorded by a gyroscope during flight. Imagery is then tied to a UTM map projection by: a) selection of ground control points (GCP's) on the reference map; b) application of the reference map coordinates of the control points to the image; and 3) warping of the image to fit the control points.. A total of 84 ground control points were registered for the four flight lines used in the image mosaic. The root mean square (rms) error for the GCP's was 9.7 meters with a standard deviation of 3.3 meters. The process of warping can improve the spatial accuracy around the control points of the image, but can degrade accuracy elsewhere, particularly at image edges or in an area with few control points. In addition, any error found in the reference map will be transferred to the image, along with the human error associated with selecting ground control points and determining coordinates (Lillesand and Kiefer 1987). The 9.7 meter rms error is the most optimal spatial accuracy assessment for this imagery, but is only applicable to the ground control points and the rest of the imagery is most likely less accurately tied to the UTM projection.

Random spatial error in excess of 10 meters is inherent in this imagery due to errors in the gyroscope data used to correct for airplane pitch and roll. Some scan lines in the flight lines became distorted when the gyroscope correction values were affected by electrical noise in the aircraft navigation system. Scan lines obviously offset by the gyroscope error were not used in

spatial accuracy assessment. The process of mosaicking the flight lines together also introduces spatial error, evident in areas where coastlines do not match exactly (Figure 4).

Figure 4 also shows the geometric distortions due to the gyroscope and distortions which are artifacts of mosaicking the different flight lines. Ideally roads should be straight and there should be no offsets of the coastlines.

The geocorrection accuracy could ideally improve to five meters if differential GPS positions were available and applied to the image data, a procedure currently in the experimental stage for airborne digital data. Cosandier et al. (1992) report only partial success integrating GPS into the CASI data stream at an accuracy of 30 to 100 meters, citing problems with GPS data collection.

## 4.3. Ground Truth

Ground truthing was accomplished during two days of hovercraft and foot surveys August 1 and 2, 1992. These surveys referenced vegetation samples and field notes to differentially corrected GPS positions, accurate to <10 cm. (This accuracy is above the requirements of this project and is because use of the hovercraft was contingent on completing another survey requiring centimeter level accuracy). GPS-referenced samples were predominantly sedge, cattail, and bulrush, along with forest and willow, and lesser vegetation including arrowhead and soft rush. One half of the GPS positions were reserved for an absolute spatial accuracy assessment of the

maximum likelihood classification. As a complement to the survey, several visits were made to accessible areas of Ladner Marsh over the course of two years. These visits provided a familiarity with the vegetation and its growth patterns which, in the end, was vital to image interpretation. The classified map was field tested by surveys made on foot guided, by the imagery. Field test were conducted in Ladner Marsh in March and July of 1994.

Color airphotos of the estuary (1:6,000) exposed May 3, 1992 were used to extend ground truthing samples from accessible to inaccessible areas, an approach recommended for wetlands by Savastano et al. (1984). The increased spatial resolution made detection of drift logs possible, as well as small or linear man made features such as training walls and wooden docks. Some fine details of vegetation canopy not evident in the CASI imagery, such as the circular stands of pioneer cattail, were also evident in the color airphoto. The advantage of using CASI imagery for production of a classified map lies in the spectral dimension and the digital format of the imagery. A digitized color airphoto would provide only three wide, overlapping spectral bands.

# 5. ANALYSIS OF MULTISPECTRAL IMAGERY

## 5.1. Spectral response patterns

Multispectral imagery for habitat mapping requires spectral response information in the visible and NIR about each species and area included in the classification. A brief introduction of spectral response patterns follows; for an in-depth discussion of energy-matter interactions in remote sensing the reader is referred to Gates et al. (1965), Hoffer (1978), Horler et al. (1983), and Lillesand and Kiefer (1987).

A surface is defined as a homogeneous area on the earth's surface within the spatial resolution of the instrument. Surfaces reflect, radiate, and/or transmit incident energy selectively at different wavelengths of the electromagnetic spectrum. The sun is the chief source of incident energy in the visible and near infrared range. The peak wavelength of incoming solar radiation is in the green visible range at approximately 540 nm (Colwell 1974).

A spectral response of a surface such as a vegetation canopy can be quantified by measuring radiance at selected wavelengths in the electromagnetic spectrum. A homogeneous surface will exhibit a characteristic trend across the wavelengths of the electromagnetic spectrum, referred to as the spectral "signature." Knowledge of the spectral signature of a surface can be used to highlight and map all areas in an image which exhibit a matching spectral response. However, as Hoffer (1978) points out, "Unique, unchanging spectral signatures do not exist in the natural world."

The shape of the observed spectral signature is a function of the sensing instrument and variations in the surface itself, the surrounding environment, and the intervening atmosphere.

Error in measurements from optical sensing instruments is attributed to sensor calibration errors, limits in sensor resolution, and errors in signal digitization. Atmospheric interference includes attenuation, path radiance, and variations in incoming solar radiation angle and intensity (Curran and Hay 1986).

Figure 5 illustrates a typical spectral signature for healthy green vegetation in the visible, near infrared, and mid infrared range. In the visible region, absorption and reflectance of light by leaf pigments defines spectral response, and in the near infrared response is determined by the cellular structure of the plant. In the mid infrared, beyond the range of the South Arm Estuary bandset, the water content of the plant and atmospheric water absorption determine spectral response (Gates et al. 1965, Hoffer 1978).

Chemical and morphological variations that take place on a daily or seasonal basis during a plant's lifetime affect spectral response patterns . The visible spectrum response (450 to 650 nm) of living vegetation is determined by the pigments present, represented chiefly as chlorophyll *a*, *b*, and *c* concentrated in the plant leaves (Bartlett and Klemas 1981, Hoffer 1978). Chlorophyll, the dominant pigment in green vegetation, absorbs from 450 to 650 nm and at 685 nm, with an absorption minima (referred to as a "reflectance peak") at approximately 540 nm, the same region as the peak wavelength of incoming solar radiation (Hoffer 1978). Thus the visible spectral signature of

Leaf
pigments

Cell
structure

Water content

} Dominant factor
controlling leaf
reflectance

80
70
60
50
40
30
20
10
0

Reflectance (%)

Chlorophyll
absorption

Water
absorption

0.4  0.6  0.8  1.0  1.2  1.4  1.6  1.8  2.0  2.2  2.4  2.6
Wavelength ($\mu$m)

Visible

Reflective infrared

Blue  Green  Red

Near infrared

Middle infrared
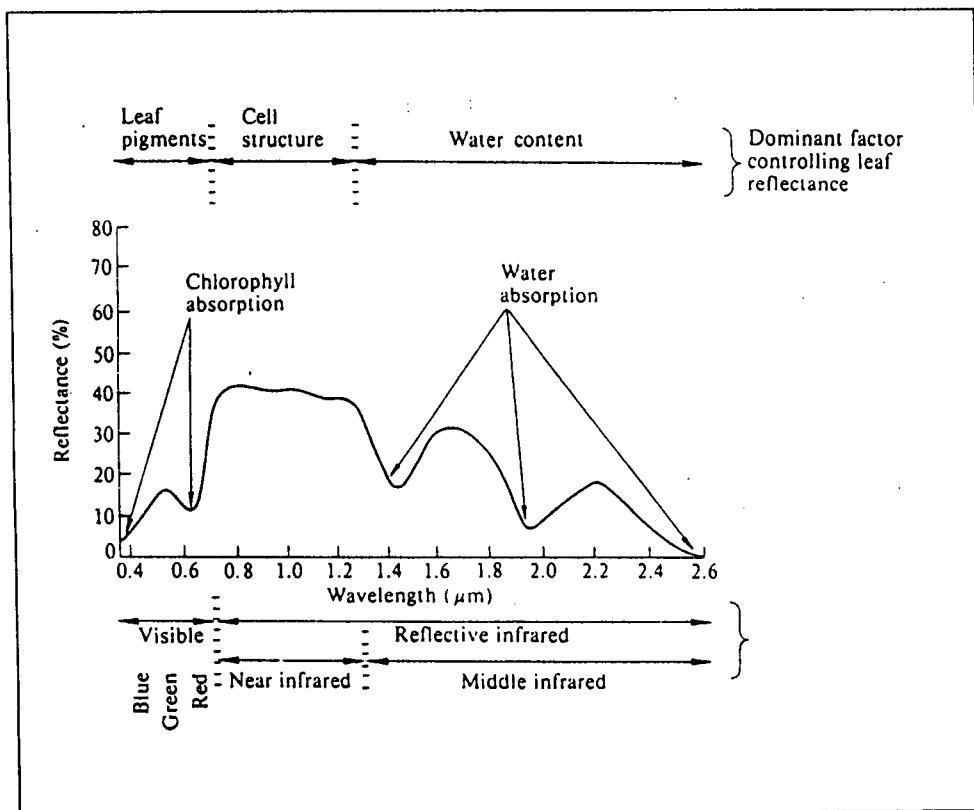
**Figure 5.** Spectral response of healthy green vegetation in the visible, near infrared, and mid infrared regions of the electromagnetic spectrum. CASI is sensitive to the 403-913 nm range (.403-.913 $\mu$m). Visible spectrum response is dominated by leaf pigments, particularly chlorophyll; near infrared response is determined primarily by cell structure; mid infrared response is related to moisture content. (From Hoffer 1978).

healthy green vegetation exhibits deep pigment absorption wells in the blue and red region and a peak in the green region. As vegetation ages, chlorophyll disappears and the green reflectance peak shifts towards the red (Gates et al. 1965). Other pigments previously masked such as carotene (orange), xanthophyll (yellow), and anthocyanin (red), become visible in the plant leaf as absorption of light by chlorophyll decreases.

The visible red (600-700 nm) spectral response of vegetation has been shown to be sensitive to vegetation canopy and cellular structure, proportion of live to dead biomass, and vegetation stress (Colwell 1974, Drake 1976, and Budd and Milton 1982). Stressed vegetation or a canopy which contains dead biomass results in reduced chlorophyll absorption, hence an increase in red reflectance (Reimhold et al. 1973).

In the near infrared (NIR), 680-1300 nm, vegetation reflectance increases to 40-60 % of the incident energy; the most rapid rise occurs between 680 and 720 nm, called the "red edge" or "red shoulder" of vegetation spectral response (Lillesand and Kiefer 1987). The NIR spectral response is determined chiefly by the morphology of the vegetation canopy, and is positively correlated with leaf area and canopy density, and negatively correlated with moisture content and necrotic biomass (Tucker and Miller 1977, Bartlett and Klemas 1981, Hardisky et al. 1984). The NIR is often used (with varying degrees of success) in vegetation biomass studies utilizing the NIR:red ratio, including Colwell (1974), Drake (1976), Tucker (1979), Bartlett and Klemas (1981), Budd and Milton (1982), Christensen et al. (1989) and Penuelas et al. (1993) . In general, the ratio is used to estimate the percentage of green vegetation by achieving a high value for the ratio when

viewing healthy vegetation (Table 2). However, as Drake (1976) points out, the ratio does not indicate the contribution of each band, only the relative relationship between the two bands. The relationship has been found to degrade when sensing a vegetation with a high percentage of stressed or dead biomass, exposed soil, or a vertically growing canopy (Reimhold et al. 1973, Bartlett and Klemas 1981, Curran 1982, Budd and Milton 1982).

The soil background will affect the spectral response of a vegetation community, particularly where the vegetation cover is sparse or the vegetation grows vertically (Tucker and Miller 1977 and Colwell 1974). Soils absorb or reflect energy depending on moisture content, organic material content, presence of iron oxide, particle size and roughness, and the proportion of sand (the dominant particle size in the Fraser River), silt, and clay (Hoffer 1978). Figure 6 shows spectral response of sand of differing degrees of saturation. Soil shows a higher reflectance in the visible region compared to vegetation, but reflection is reduced with an addition of moisture. Bartlett and Klemas (1981) report no correlation of soil spectra and vegetation biomass in the visible region in the wetland environment, attributed to dark and saturated soils. However, Tucker and Miller (1977) found that soil spectra dominated low grass canopies, and the soil spectra contribution in the NIR is inversely related to biomass or vegetation density . Hardisky et al. (1984), working in a salt marsh, found soil spectra to degrade the NIR:red ratio by increasing visible red response.

Some chemical deficiencies will increase plant reflectance in the visible red and NIR, namely deficiencies of nitrogen, potassium, phosphorus,

**Table 2.** Spectral relationships relevant to the NIR:red ratio for vegetation biomass estimation. All relationships result in a high contrast ratio, diminishing the effectiveness of the ratio for green biomass estimation.

| Remotely sensed surface | Near infrared reflectance | Visible red reflectance |
|---|---|---|
| Green healthy vegetation | high | low |
| Necrotic biomass | low | high |
| Vegetation with vertical canopy | low | high |
| Soil | low | high |
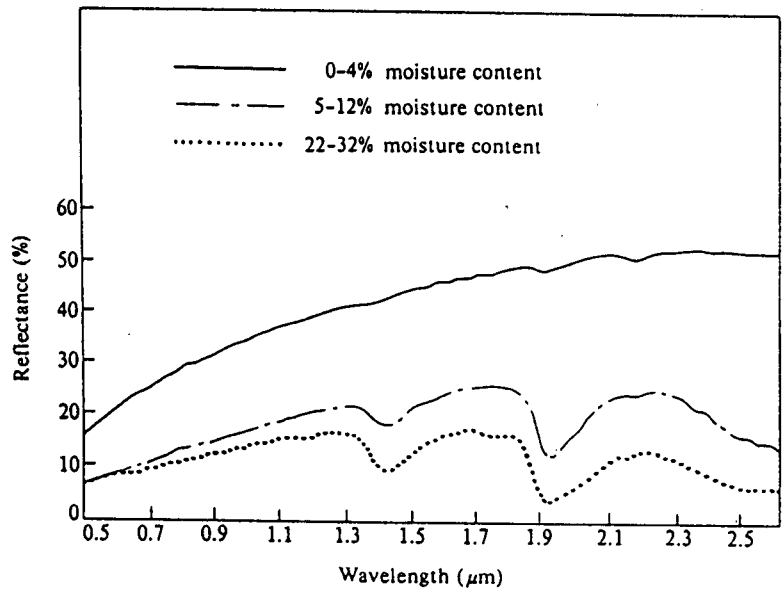
**Figure 6.** Spectral response of sand of differing degrees of moisture saturation. The Fraser River is a sand dominated river. An increase in moisture decreases reflectance in the visible, near infrared and mid infrared. Water absorption bands are seen at 1.4 μm and 1.9 μm. (Note CASI sensitivity range of .403- .913 μm). (From Hoffer 1978).

magnesium, calcium, and sodium. Salt stress can change the chlorophyll and carotenoid concentrations in plants (Reimhold et al. 1973 and Bracher 1991).

The vegetation canopy can also be physically altered in the wetland environment by wind and water. Bartlett and Klemas (1981) note stems and leaves flattened by wind and water have a decrease in NIR response. Flattened cattail, bulrush, sedge, and grass (*Agrostis spp.*) were observed during ground truthing (July and August 1992) at the waterline and in drainage channels.

## 5.2. Spectral response generation

A supervised classification is a mapping procedure for land cover types which uses the spectral response of areas of interest to train a computer algorithm to identify like pixels in a digital image. Ground truthing is required to correlate the composition of an area on the ground with a location in the image. The area identified in the image is delineated as a "training area" representing a population in the classification. The mean digital number for each band of image data for each training area is generated and used to customize the supervised classification algorithm. The algorithm examines each pixel in an image for radiances similar to those of the training areas (within three standard deviations of the mean digital number) and classes them appropriately. The pixel is classed as null class if no match is found.

Histograms of pixel brightness are used to evaluate the distribution of radiance in a training area. A bimodal histogram indicates the presence of two populations in a training area, and a scattered histogram indicates multiple populations in a training area. Both bimodal or scattered histograms can be acceptable, particularly at class or habitat boundaries. Training areas are also evaluated in the confusion matrix, which provides a report of the training areas' performance in the final classification.

The maximum likelihood classification relies on ellipsoids of equiprobability around the signature in n-dimensional space, where the number of dimensions equals the number of bands used in creation of the spectral

signature. All pixels falling in an ellipsoid belong to that class. Pixels which do not fall in the range of an ellipsoid are classified as null.

The range and shape of the ellipsoids are critical to the classification. The shape of an ellipsoid is affected by overlapping ellipsoids, and inclusion or exclusion of signatures will affect the classification. The size and shape of a signature's ellipsoid is determined by: the number of bands used in the signature, the number of pixels in all bitmaps used to generate the signature, and the shape and size of ellipsoids of adjacent signatures.

The process of identifying ground truth, delineating training areas and generating characteristic spectral signatures for each population in the classification is a time consuming and iterative process. Each class for the classification must have at least one training area, and often more are required to account for variation within a species or environment, and variation in the data collection process. The delineation of training areas is subject to analyst interpretation and the radiance distribution in each band is assumed to be Gaussian. If the spectral response of a vegetation or substrate is not specifically known (which is often the case) or if ground truth is not gathered, it is possible that two analyses of the same image could produce a very different map. The characteristic spectral responses generated from the training areas provide the blueprint for the classification of the entire image, and the quality of the training areas determine the quality of the classification (Lillesand and Kiefer 1987).

## 5.3. Classification signatures

Spectral response signatures were collected from the training areas for the classes discussed in Section 3. Spectra for forest, willow, cattail, sedge, and bulrush are presented in Figure 7 and spectra for tidal flat, necrotic biomass, and drift logs are shown in Figure 8. A covariance matrix can be used to determine which bands contain less correlated information (and hence higher image contrast). Bands 1 (450-503 nm) and 6 (658-670 nm) were excluded from the signature generation and classification because the spectral radiance values were highly correlated with other bands and contained little discriminating information. Band 11 (861-879 nm) was excluded from analysis because of saturation of the instrument's radiance detectors during data collection. Bands which contain less correlated information (as determined by the covariance matrix) include Band 3 (545-556 nm), Band 5 (632-643 nm), Band 7 (671-686 nm), and Band 10 (748-754 nm).

Spectral response follows patterns discussed in Section 5.1. The chlorophyll reflectance peak is seen in Band 3 (545-556 nm), while chlorophyll absorption is evident in the blue and red visible region, particularly Band 7 (671-686 nm). For bulrush, the reflectance peak is depressed and the red visible response is increased relative to the other vegetation classes because of the background contribution of the soil. Small chlorophyll reflectance peaks are seen in Band 3 in the unvegetated classes, indicating some degree of green biomass is present. The response between Band 7 at the edge of the red visible and Band 8 (687-698 nm) at the beginning of the near infrared shows an increase for all vegetation except bulrush, and a decrease for all non-vegetated classes. The factors degrading the NIR:IR ratio are seen: dead biomass,

35
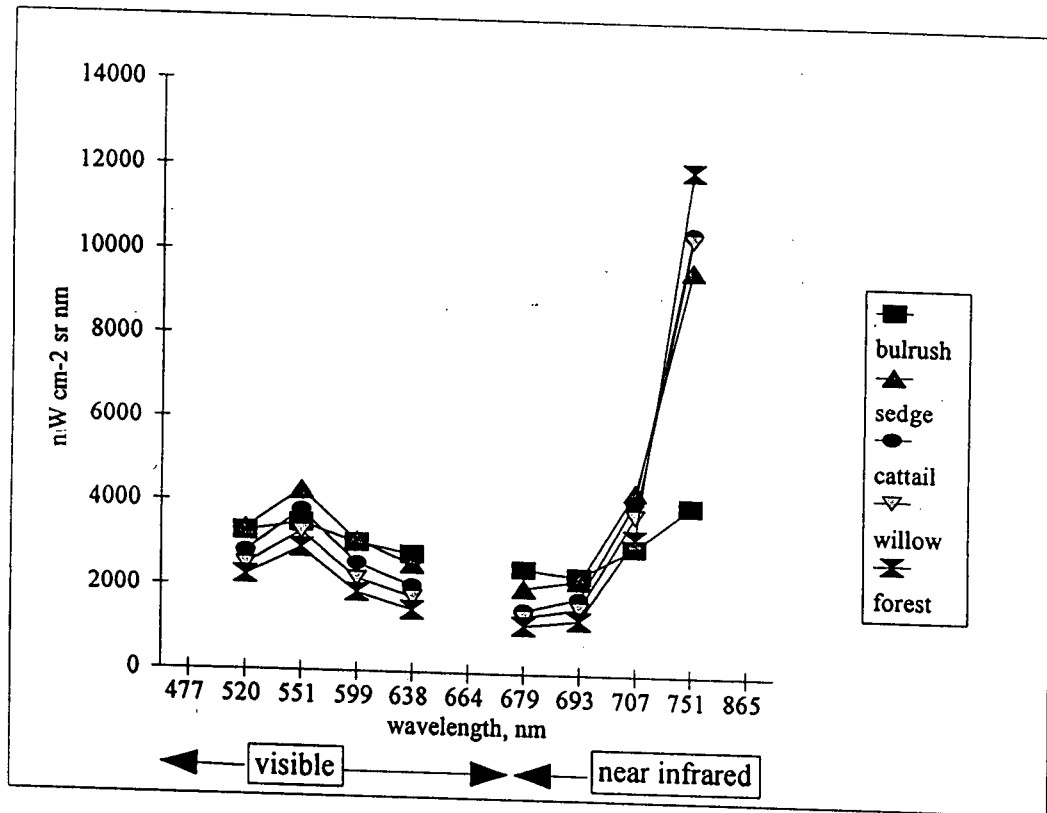
**Figure 7.** Spectral response of vegetation categories. Note categories represent vegetation communities dominated by a single species. Categories contain the effects of intermixed and adjacent vegetation and / or soil and water backgrounds.
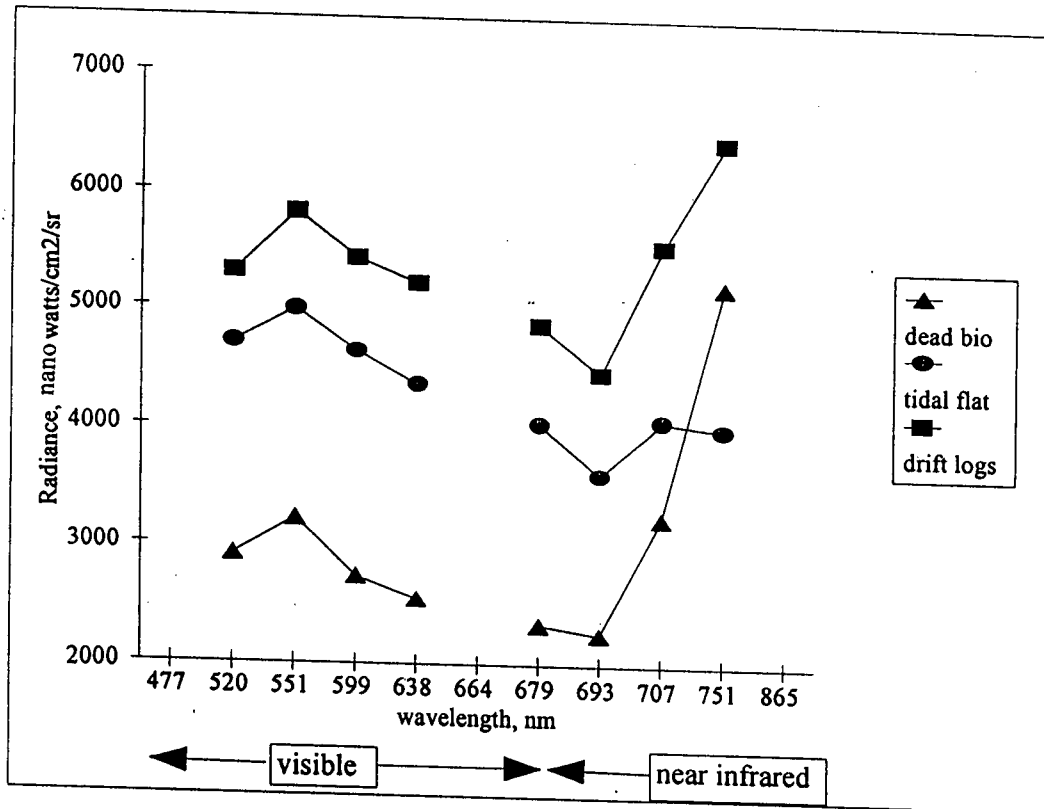
**Figure 8.** Spectral response of dead biomass and non-vegetated areas. Drift logs and tidal flats show a high reflectance in the visible. The low NIR response of tidal flat areas is attributed to potholed water on the flat and to adjacent water bodies. Dead biomass has a form similar to vegetation but exhibits a depressed chlorophyll reflectance peak and a much lower NIR response.

exposed soil (tidal flat), and vertical canopy (bulrush) show an increase in the visible red which, coupled with the reduction in the NIR, provides a high contrast ratio. Healthy green vegetation, which has a a low red visible and high NIR response, also exhibits a high contrast ratio. Hence, the NIR:red ratio will not necessarily discriminate between a healthy canopy and a canopy with a soil or necrotic biomass background.

The influence of canopy is illustrated in the NIR, with the highest response from forest, the next highest from willow and cattail, followed by sedge and a low return from the vertical bulrush canopy. Dead biomass and drift logs show an increased reflectance in the NIR, attributed to the presence of some amount of living vegetation. The depressed NIR response for the tidal flat is attributed to the presence of water on the tidal flat, as water absorbs strongly in the NIR.

The most similar spectral signatures belong to cattail and sedge. Of eight cattail and four sedge samples identified by ground truthing, the defining relationship is a lower visible and higher NIR response for cattail, illustrated in Figure 9. Both species grow in similar environments, often in conjunction with the same plant species, which compounds difficulties in spectral discrimination. An unsupervised classification would not delineate between them, as differences in the signature are small and the standard deviations of the signature means overlap. However, based on the supervised classification results, some discrimination or habitat zonation was achieved. Figure 10 shows the classification results for Ladner Marsh for the two species. Bulrush (purple) represents vegetation growing at the lowest
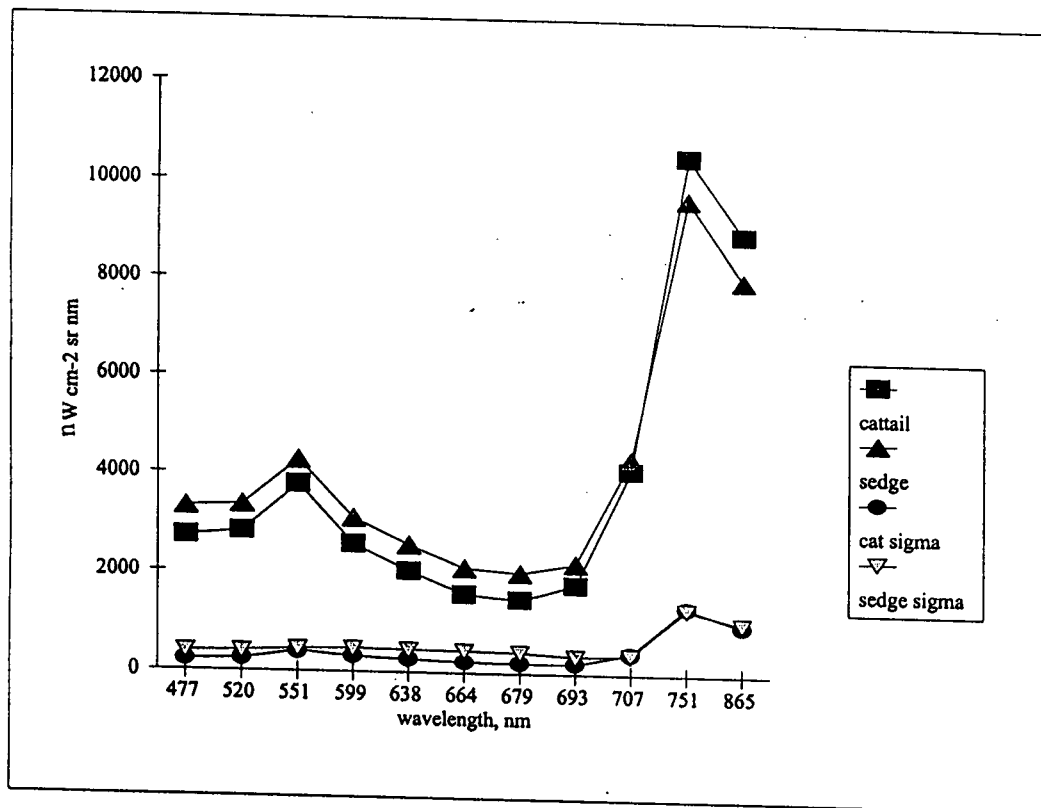
**Figure 9.** Spectral response of cattail and sedge communities. A total of eleven cattail and sedge samples were examined and the most well defined difference is a lower visible and higher NIR response for cattail respective to sedge.
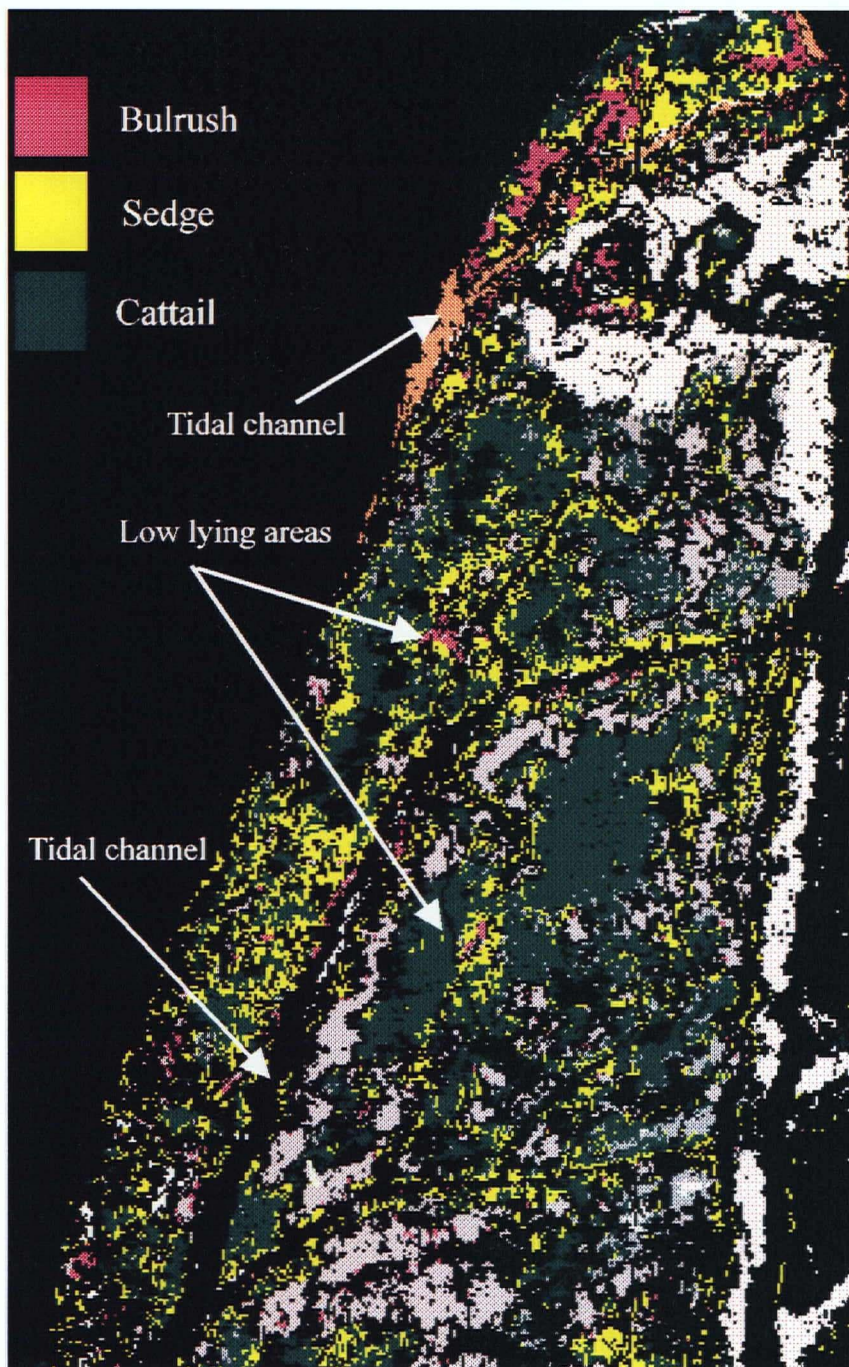
Figure 10. Supervised classification results for cattail and sedge
communities illustrating differentiation, despite similar spectral reponse.

40

elevations, sedge, seen in yellow correlates with tidal channels and lowland areas, adjacent to stands of bulrush. Cattail, in green, is seen at higher elevations in more dense stands.

Classification results for Ladner Marsh, Kirkland and Gunn Islands and portions of Duck and Barber Islands are presented in Figure 11. The mouth of the south arm of the Fraser River is to the left of the image. Forest is found on the highest ground and is associated with agricultural areas which have been stabilized by training walls (Moody 1978). Willow is often intermixed with forest. The lower marsh vegetation follows the zonation associated with tidal range and drainage where bulrush is found in low lying areas and adjacent to tidal flats, sedge is found at slightly higher elevations and lining tidal channels, and cattail is associated with sedge but often at higher elevations (Kistritz 1990). A significant amount of dead biomass has collected in Ladner Marsh and on Barber Island (Mark Adams, pers. comm. 1994).
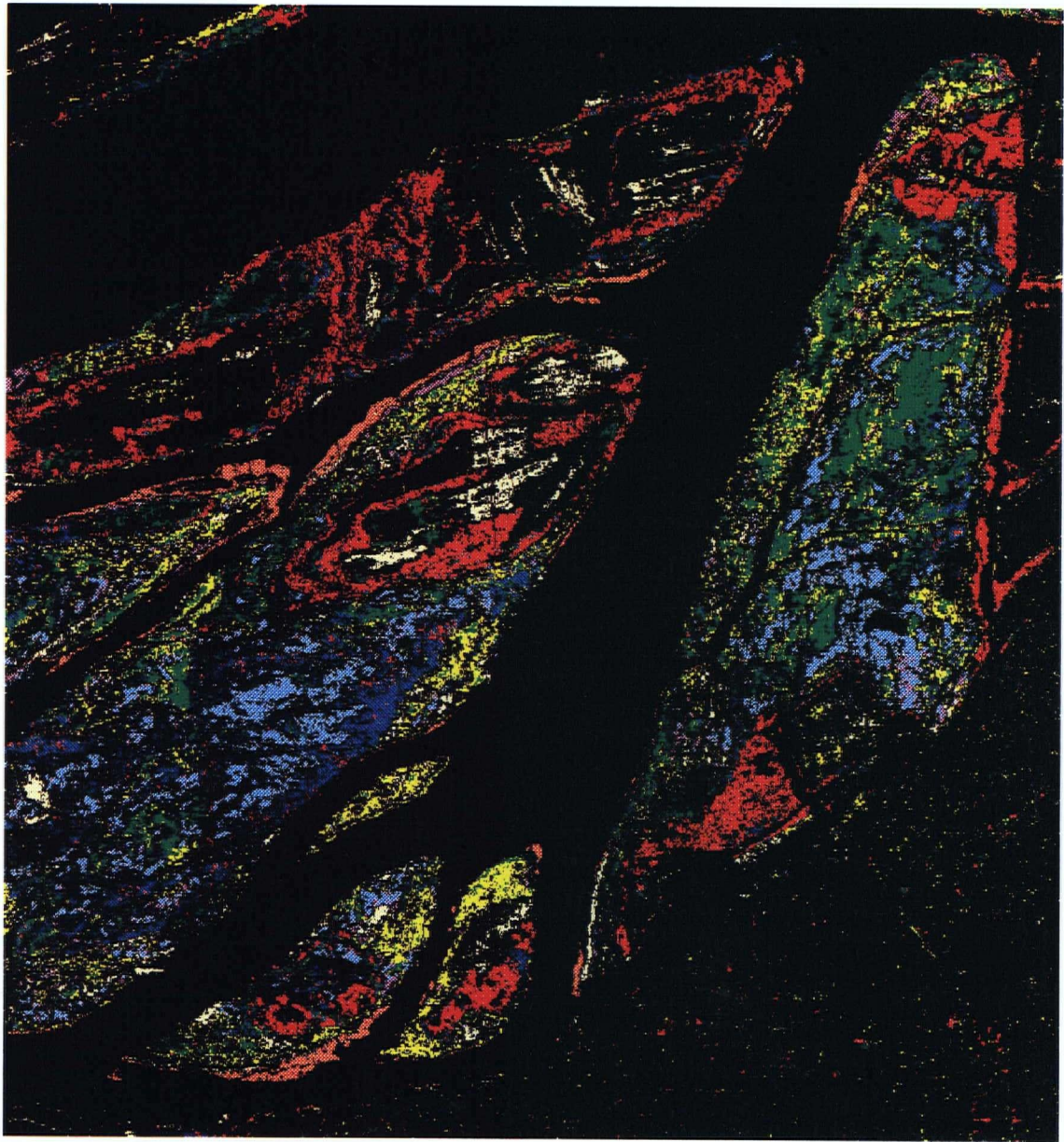
Fig. 11. Classification results. Red=forest, dark blue=willow, green=cattail, yellow= sedge, purple=bulrush, light blue=dead biomass, gray=drift logs, tan=tidal flat, white=drift logs.

42

Training areas which include several different populations result in spectral signatures which are averages of those populations. A nonspecific or generic signature will tend to classify scattered areas across the image. This was particularly evident when attempting to classify agricultural areas in the image. Because of the small scale of the agriculture, different crop types and areas left fallow, the agricultural signature was more like an average of many responses. Even when training areas were made selectively, the signature for the agricultural areas tended to classify pixels all over the image. Hence the agricultural signature was not used. Some of the agricultural lands are classified as drift logs in the final classification. The poor classification result is not uncommon for agriculture due to different crop types, seed varieties, planting dates, soil moisture, and topography (Lillesand and Kiefer 1987).

## 6. RESULTS and DISCUSSION: MAP ACCURACY

This discussion focuses on the accuracy or confidence level of the classification results seen in Figure 11. Used for analysis are an error matrix, field tests of the classified map, and comparison with GPS-referenced ground truth samples.

## 6.1. The Error Matrix

An error matrix (also called a confusion matrix) presents the individual accuracies of each training area in a meaningful tabular format. The matrix is a pixel by pixel break down of the performance of each training area in the final classification. An error matrix provides confidence levels for the integrity of each training area and thus the spectral signature generated from it. To account for species and spectral variance in the different flight lines, classification categories have spectral signatures derived from more than one training area. Table 3 presents the results from the error matrix for the supervised classification of the South Arm Estuary. Weak training areas contain many differently classified pixels, or a large amount of pixels classified as null. In addition, overlap between categories is highlighted. Incorrectly classed pixels are not a random mistake, but tend to class in a category with a similar spectral response. Category overlaps are due to similar spectral response or similar growth distribution in the environment. Bulrush and dead biomass show some confusion (4.8% in the dead biomass training areas, 1.1% in bulrush training areas). Both categories are found in low lying areas and both signatures have lower NIR responses than dense green vegetation. Interestingly, the low NIR response for bulrush is attributed in part to its

44

**Table 3.** Error matrix providing user and producer accuracy estimates for training areas used in the supervised classification. The matrix represents a pixel by pixel breakdown of each training area and indicates how well the training areas performed in the final classification. (One pixel is equal to a 3.5 m$^2$ area).

| | rush | sedge | cattail | willow | forest | dead bio | drift logs | tidal flat | null class | row total | train. area user acc., % | class user acc., % |
|---|---|---|---|---|---|---|---|---|---|---|---|---|
| wood 1 | | | | | | | 548 | | 137 | 685 | 80 | 82 |
| wood 2 | | | | | | | 210 | | 42 | 252 | 83 | |
| tidal flat 1 | | | | | | | 3 | 424 | 119 | 546 | 78 | 81 |
| tidal flat 2 | | | | | | | 8 | 1996 | 395 | 2399 | 83 | |
| dead bio 1 | 21 | 4 | | 1 | | 828 | | | 183 | 1037 | 80 | 74 |
| dead bio 2 | 90 | 6 | | | | 869 | | | 312 | 1277 | 68 | |
| rush 1 | 277 | 4 | 1 | | | 11 | | 4 | 76 | 373 | 74 | 76 |
| rush 2 | 1242 | | | | | 10 | | | 342 | 1594 | 78 | |
| sedge 1 | 3 | 691 | 107 | 1 | | | 3 | | 214 | 1019 | 68 | 70 |
| sedge 2 | | 301 | 65 | | | | | | 124 | 490 | 61 | |
| sedge 3 | | 47 | 1 | | | | | | 9 | 57 | 82 | |
| cat 1 | | 11 | 547 | 9 | | | | | 49 | 616 | 89 | 77 |
| cat 2 | | 11 | 533 | 26 | 9 | | | | 154 | 733 | 73 | |
| cat 3 | | 11 | 369 | 1 | | | | | 109 | 490 | 75 | |
| cat 4 | | 18 | 257 | 3 | 5 | | | | 72 | 355 | 72 | |
| willow 1 | | 1 | 6 | 421 | 10 | | | | 85 | 523 | 81 | 75 |
| willow 2 | | 4 | 50 | 895 | 68 | | 1 | | 277 | 1295 | 69 | |
| forest 1 | | 9 | 6 | 31 | 1303 | | | | 212 | 1561 | 83 | 76 |
| forest 2 | | 2 | 29 | 122 | 3645 | | | | 1200 | 4998 | 73 | |
| forest 3 | | | 26 | 67 | 1218 | | | | 381 | 1692 | 72 | |
| column total | 1633 | 1120 | 1997 | 1577 | 6258 | 1718 | 733 | 2424 | 4492 | 21992 | | |
| producer acc. % | 93 | 93 | 85 | 83 | 99 | 98 | 98 | 100 | | | | |

colonization of tidal flats and the influence of the soil background, but the matrix shows virtually no confusion between the bulrush and tidal flat signature. The tidal flat training areas do contain a small percentage of drift log pixels (0.4%), attributed to the presence of drift logs deposited on tidal flats. Forest training areas are confused with willow 2.7% and cattail 0.1%. Willow overlaps forest 4.3% and cattail 3.0% . Cattail overlaps sedge 2.3%, willow 1.8%, forest 0.6%. Sedge overlaps cattail 11%, rush 0.2%, and wood 0.2%. Bulrush overlaps 1.1% with dead biomass, 0.2% with sedge, and 0.2% with tidal flat. Dead biomass overlaps 4.8% with bulrush, 0.4% with sedge.

Two different estimates of accuracy are made from confusion matrices: producer's accuracy and user's accuracy. Producer accuracy is defined as the probability that a reference sample is correctly classified. Of eight categories, seven had a producer accuracy of 93% or higher, and four categories were 98 to 100% accurate. Producer accuracy is too high to be of use in an accuracy assessment. This approach ignores errors of omission, where a pixel is classified as null. User accuracy is defined as the probability that a site visited will contain what the classified map indicates. This estimate includes errors of omission in the null class and errors of commission which result from spectrally similar classes or vegetation closely associated in the environment. User accuracies of classification categories accuracies ranged from 70% to 82%. The user accuracy of individual training areas ranged from 61% to 89%. The less homogeneous categories, sedge and dead biomass scored lowest (70%, 74% respectively), while unvegetated categories, wood and tidal flat scored highest (82%, 81% respectively).

46

Null classification averaged 20% for the categories. It is very possible that heterogeneity in the marsh is such that a higher accuracy is not possible, because a 100% vegetation cover or homogenous area does not exist in the marsh. A high amount of shadow exists in forested areas and probably contributes to the null classification of 22%. (Colwell 1974). Sedge is also 22% null, which is attributed to many associated species and to a lesser extent variability in the growing environment.

This approach to accuracy assessment is independent of the spatial errors in the image because training areas were identified using relative methods, such as field identification of a homogeneous patch of vegetation referenced to a conspicuous feature (a wooden observation tower in the marsh, a confluence of drainage channels) or by airphoto interpretation. GPS-referenced points were not used to identify training areas because the GPS points do not directly overlay the geocorrected image.

## 6.2 Field Test of Classified Map, Spring and Summer

Two field tests of the classified map were conducted in Ladner Marsh in May and July of 1994. Fourteen sites were visited (Figure 12) and visually inspected for forest, willow, cattail, sedge, and tidal flat. Of the 14 sites, 11 were correctly classified resulting in a field test accuracy of 78.5%. The choice of sites relied on the identification of areas visible and distinct in the imagery, such as areas adjacent to an observation tower, an old sewage pond, drainage channels, and man made trails and roads. In addition, sites were as chosen as representative of all populations in the classification and for ease of access. A correct classification identifies the dominant population of the site. The minimum ground area of a site is equal to the square of the pixel size, although consideration was given for vegetation such as bulrush which tends to grow linearly.

Most of the confusion is related to a collection of unflushed necrotic biomass underneath a healthy cattail community at site A. Visits to Ladner Marsh in the winter located the dead cattail stands which are obscured by live cattail in July. It is a matter of opinion if this is a misclassification or an appropriate mapping of marsh hydrologic regime.

The tip of the marsh near L is a low marsh area, bounding the main river channel, densely populated by cattail at higher elevations and sedge and bulrush at lower elevations. However, several pixels were misclassified as forest due to a high NIR response.
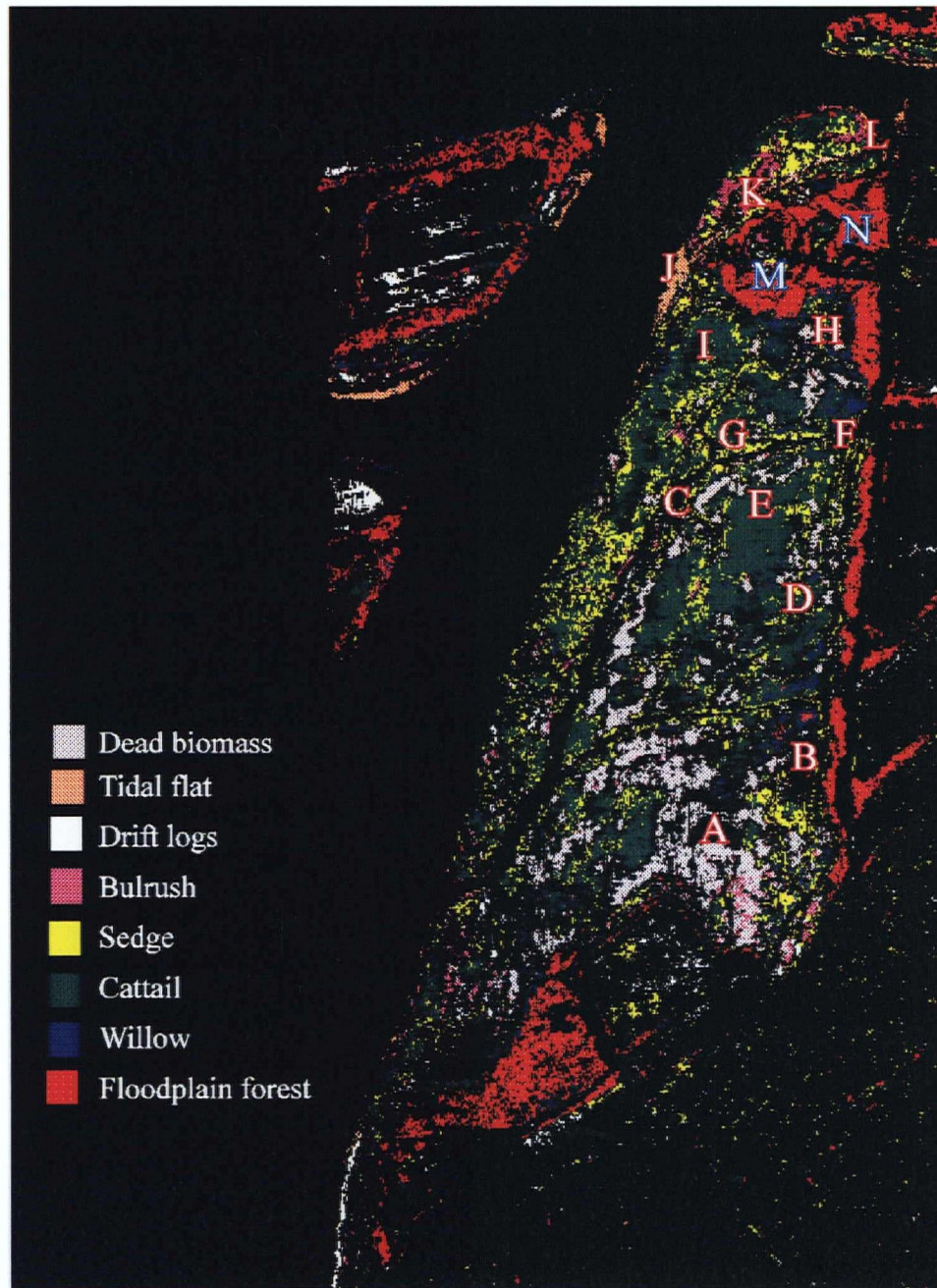
Figure 12. Sites visited in Ladner Marsh for field test of classified map, spring and summer.

49

Willow along the main tidal channel at site B did not classify well, although willow did classify well at near the waterline near site I and in areas of higher elevation.

Dense stands of purple loosestrife approximately 2-4 pixels or more were identified in the field at site I, and are seen as a null classification at the moment. Attempts to separate the loosestrife from the sedge and cattail have not been successful as of yet.

All other classes were found to be accurately represented on the classified map. One interesting area is found at N. The area at site N floods during high tide, leaving most of the vegetation covered with silt. This lessens overall radiance (Gross and Klemas 1986), yet several pixels classified correctly as bulrush and sedge.

The field test is similar to the user accuracy assessment of the confusion matrix in that it answers the question "What is the probability that a site visited in the field corresponds to that of the map?". The difference is that user accuracy derived from the confusion matrix is limited to the training areas, whereas the field test assesses a larger area, much of which has not been ground truthed. The disadvantage of the field test is that it relies on visual identification of a generalized area.

## 6.3 The Vegetation Index

The vegetation index was employed in the form of the simple ratio (NIR/red) and the Normalized Difference Vegetation Index, or NDVI (NIR-red/NIR+red) to further investigate the misclassification at site A (Figure 12). No significant difference in results were seen between the simple ratio and the NDVI. The NDVI results, shown in Figure 13, confirm the dependence of the vegetation index on dead biomass, silt covered vegetation, and soil background. The most dense vegetation is colored green, less dense yet healthy vegetation is yellow, and areas with a low vegetation index are seen in red.

The lower portion of the marsh populated by dense cattail did not perform favorably in the vegetation index. The presence of dead biomass underneath the live cattail increased the visible red response (where chlorophyll usually absorbs) and decreased the NIR response (which is high for dense healthy vegetation). Necrotic biomass can be 40% or more in a wetland environment (Bartlett and Klemas 1981) and the vegetation index can be used to detect concentrations of necrotic biomass which may be hidden under a healthy canopy.

Vegetation covered by silt during the tidal cycle is another factor complicating classification and biomass estimation in wetland environments. The area designated in Figure 13 is inundated by tide twice a day and vegetation is layered with silt, which increases the visible red and decreases the NIR response of vegetation. The supervised classification was more successful in detecting live silt-covered vegetation, seen in Figure 11.

Silt covered vegetation

Dead biomass under healthy cattail
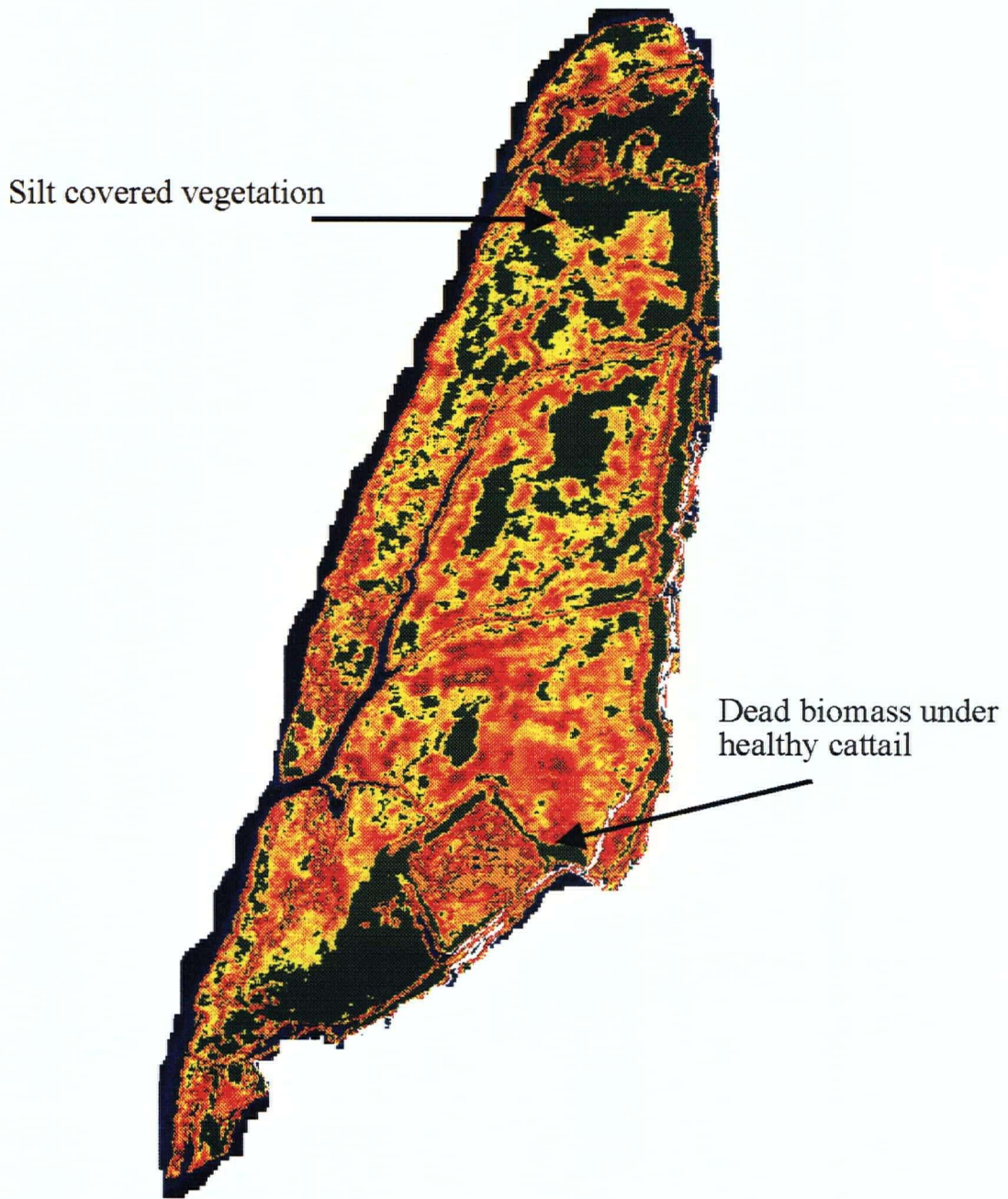
Fig. 13. Vegetation index for Ladner Marsh (NIR-red/NIR+red). NIR=bands 10,11, red=bands 7,8. Green and yellow are dense vegetation, red areas have low index value.

52

## 6.4. Spatial Agreement with Spatially Referenced Ground Truth

To evaluate spatial accuracy of the classification GPS-referenced ground truth positions were plotted on the UTM grid and compared with the classified image map. It is currently popular to use the Global Positioning System (GPS) to locate ground truth. A site can be visited, identified, and referenced to a fixed coordinate system, then used in identification of training areas or post-classification accuracy assessment. However, GPS-referenced ground truth is only useful in very accurately geocorrected images.

The results are summarized in Tables 4-6 for cattail, sedge, and bulrush ground truth samples. Of 13 samples, cattail showed an average spatial error of 5.8 pixels, or 20.4 meters. The 13 sedge samples indicate an accuracy of 4.1 pixels, or 14.4 meters. Bulrush had the lowest accuracy of 23.4 pixels, or 53.3 meters for 8 samples. Cattail and sedge are widely dispersed in the marsh and their accuracy may be artificially high due to a high frequency of occurrence in the marsh, i.e. the chance that an overlain ground truth sample will lie close to a pixel classified as that category increases as the total number of pixels in the category increases. Bulrush, a more localized species, will be less likely to coincidentally overlap with the ground truth and 53 meters is accepted as the spatial accuracy of the classification.

There are few studies addressing the spatial and geometric accuracy of airborne MSS data (Christensen et al. 1989, Jensen et al. 1986). Geocorrecting airborne multispectral imagery is problematic (due in most part to the motion of the aircraft) and the lack of precise base maps for coastal environments. In summary, spatial errors in multispectral imagery are

**Table 4.** Spatial agreement between classified image and GPS referenced ground survey positions of cattail in Ladner Marsh.

| Cattail ground survey point | Number of pixels to nearest correctly classified pixel | Meter distance to nearest correctly classified pixel |
|---|---|---|
| 1 | 5.0 | 17.5 |
| 2 | 16.0 | 56.0 |
| 3 | 5.0 | 17.5 |
| 4 | 4.1 | 14.4 |
| 5 | 10.2 | 35.7 |
| 6 | 10.8 | 37.8 |
| 7 | 7.1 | 24.7 |
| 8 | 10.4 | 36.5 |
| 9 | 2.0 | 7.0 |
| 10 | 2.0 | 7.0 |
| 11 | 1.0 | 3.5 |
| 12 | 1.0 | 3.5 |
| 13 | 1.0 | 3.5 |
| **Average and standard deviation** | **5.8 (4.8)** | **20.4 (16.7)** |

**Table 5.** Spatial agreement between classified image and GPS referenced ground survey positions of sedge in Ladner Marsh.

| Sedge ground survey point | Number of pixels to nearest correctly classified pixel | Meter distance to nearest correctly classified pixel |
|---|---|---|
| 1 | 2.2 | 7.8 |
| 2 | 2.2 | 7.8 |
| 3 | 9.9 | 34.6 |
| 4 | 12.0 | 42.1 |
| 5 | 0.0 | 0.0 |
| 6 | 5.1 | 17.8 |
| 7 | 10.8 | 37.7 |
| 8 | 4.2 | 14.8 |
| 9 | 3.0 | 10.5 |
| 10 | 0.0 | 0.0 |
| 11 | 3.0 | 10.5 |
| 12 | 0.0 | 0.0 |
| 13 | 1.0 | 3.5 |
| Average and standard deviation | 4.1  (4.2) | 14.4  (14.7) |

**Table 6.** Spatial agreement between classified image and GPS referenced ground survey positions of bulrush in Ladner Marsh.

| Bulrush ground survey point | Number of pixels to nearest correctly classified pixel | Meter distance to nearest correctly classified pixel |
|---|---|---|
| 1 | 5.0 | 17.5 |
| 2 | 12.0 | 42.0 |
| 3 | 18.9 | 66.0 |
| 4 | 33.0 | 116.0 |
| 5 | 26.0 | 91.0 |
| 6 | 82.3 | 82.3 |
| 7 | 5.4 | 5.4 |
| 8 | 5.8 | 5.4 |
| **Average and standard deviation** | 23.4 (25.9) | 53.3 (42.0) |

attributed to: instrument errors, variations in data collection procedures; transient nature of wetland environment; and errors in the reference information used for geocorrection. Much of the spatial error in this image is in the attitude correction of the CASI image, caused by a nonsystematic electrical noise in the gyroscope data in airplane navigation system during the flight (Borstad 1993, pers. comm.). Nonlinear distortions in an image are extremely difficult if not impossible to correct (Christensen et al. 1989).

Whereas the field test relied on areas identified relative to distinct landmarks, the GPS ground truth was collected in a coordinate system independent from the UTM grid used to geocorrect the imagery. Essentially, the GPS positions exist as points in space. Errors or offsets in the UTM reference map and/or artifacts of the image registration and mosaicking degrade agreement between GPS-referenced ground truth and the image.

# 7. SUMMARY AND CONCLUSIONS

Detection and identification of dominant vegetation species of the estuarine environment is possible with multispectral image data, and detected species and strata are indicative of the hydrologic regime. However, the development of robust training areas and spectral signatures is an iterative and intensive procedure. Because no set of standard spectral signatures exists, no "black box" or automated procedure can be substituted for the analyst. By the same token, the classified image is a direct reflection of the input.

Literature reviews and area visits help to determine the growing habits of plants, and some knowledge of spectral response patterns is needed to interpret the imagery.

Ground truthing is required to link a spectral response with a species. The most reliable ground truth is relative to a fixed recoverable point which can be seen in the imagery. This avoids the problem of having ground truth referenced with an accuracy different from the image, demonstrated with the GPS-referenced ground truth collected for this study. Absolute spatial accuracy of airborne multispectral imagery deserves more attention. GPS could be better suited for marking ground control points used to geocorrect the imagery, rather than for marking ground truth for the classification. Airphotos proved valuable in extending ground truth information to inaccessible areas and for the superior spatial resolution.

The bandset was adequate to separate vegetation communities. In the future, a field spectrometer could be used to determine spectral response of vegetation and substrate. This information could be used to configure the airborne spectrometer before data collection or to check the accuracy of signatures generated from the imagery.

The most difficult signatures to separate were of vegetation species which grow in conjunction with each other and exhibit a similar spectral response, as in the case of cattail and sedge. Further attention is needed to distinguish between the cattail and sedge. June, close to the period of peak growth, may not be the optimal time in the growing season for discrimination. Dense homogeneous stands of vegetation were the most easily identified according to spectral response, while heterogeneous communities not dominated by any particular species were difficult to quantify.

Dead biomass under a healthy vegetation canopy has an effect on the spectral response of the canopy. Dead biomass and soil background degrade the effectiveness of the NIR:red ratio for green biomass estimation but can be used to find collections of unflushed necrotic biomass.

All flight lines must be flown in a consistent direction, either towards or away from the sun. Radiometric discrepancies between flight lines compromised the accuracy of the classification and resulted in the exclusion of one flight line.

# BIBLIOGRAPHY

Anderson, John and M. Roos, 1991. Using Digital Scanned Aerial Photography for Wetlands Delineation. *Earth and Atmospheric Remote Sensing,* SPIE Vol.1492, pp. 252-262.

Anger, C.D., S.K. Babey, and R.J. Adamson, 1990. A New Approach to Imaging Spectroscopy. *Imaging Spectroscopy of the Terrestrial Environment,* SPIE Vol. 1298, pp. 72-82.

Aronoff, Stan, 1982. The Map Accuracy Report: A User's View. *Photogrammetric Engineering and Remote Sensing,* Vol.48, No.8, pp. 1309-1312.

Bartlett, David, and V. Klemas, 1981. In situ spectral reflectance studies of tidal wetland grasses. *Photogrammetric Engineering and Remote Sensing,* Vol. 47, No. 12, pp. 1695-1703.

Best, R.G., M.E. Wehde, and R.L. Linder, 1981. Spectral reflectance of hydrophytes. *Remote Sensing of Environment,* Vol. 11, pp. 27-35.

Borstad, Gary, and D. A. Hill, 1989. Using Visible Range Imaging Spectrometers to Map Ocean Phenomena. *Proceedings: Advanced Optical Instrumentation for Remote Sensing of the Earth's Surface from Space,* Vol. 1129, pp. 130-136.

Borstad, G. 1992. Ecosystem Surveillance and Monitoring With the Portable Airborne Imaging Spectrometer. First Thematic Conference on Remote Sensing for Marine and Coastal Environments, June 1992, New Orleans, Louisiana; 10 pp.

Bracher, Grant, 1991. Detection of nutrient stress in Douglas fir seedlings using spectroradiometer data. Ph D thesis, Faculty of Forestry, University of British Columbia.

Bradfield, G.E., and G.L. Porter, 1982. Vegetation structure and diversity components of a Fraser estuary tidal marsh. *Canadian Journal of Botany,* Vol. 60, pp. 440-451.

Brown, Walley, 1978. Wetland mapping in New Jersey and New York. *Photogrammetric Engineering and Remote Sensing,* Vol. 44, No. 3, pp. 303-314.

Budd, J.T., and E.J. Milton, 1982. Remote sensing of salt marsh vegetation in the first four proposed Thematic Mapper bands. *International Journal of Remote Sensing*, Vol. 3, pp. 147-161.

Butera, M.K., 1983. Remote sensing of wetlands. *IEEE Transactions on Geoscience and Remote Sensing*, Vol. GE-21, No. 3, pp. 383-392.

Canadian Wetland Service, 1987. Canadian Wetland Classification System. Ecological Land Classification Series No. 21, C.W.S. and Environment Canada, 18 pp.

Christensen, E.J., J.R. Jensen, and H.E. Mackey, 1989. Wetland vegetation change detection in the Savannah River swamp using airborne multispectral scanner data. Freshwater Wetlands and Wildlife, 1989. DOE Symposium Series No. 61, R.R. Sharitz and J.W. Gibbons, eds., pp. 1029-1043.

Colwell, Robert, 1963. Basic matter and energy relationships involved in remote reconnaissance. *Photogrammetric Engineering and Remote Sensing*, Vol. 29, pp. 271-299.

Colwell, John, 1974. Vegetation Canopy Reflectance. *Remote Sensing of Environment*, Vol. 3, pp. 175-183.

Cosandier, Darren, T. Ivanco, and S. Mah, 1992. The Geocorrection and Integration of the Global Positioning System with the Compact Airborne Spectrographic Imager, Fifteenth Canadian Symposium on Remote Sensing, June 1992, pp. 385-390.

Curran, Paul, 1982. Multispectral photographic remote sensing of green vegetation biomass and productivity. *Photogrammetric Engineering and Remote Sensing*, Vol. 48, No. 2, pp. 243-250.

Curran, Paul, and Alan Hay, 1986. The importance of measurement error for certain procedures in remote sensing at optical wavelengths. *Photogrammetric Engineering and Remote Sensing*, Vol. 52, No. 2, pp. 229-241.

Day, J., 1989. Estuarine Ecology, Wiley, New York.

Drake, Bert, 1976. Seasonal changes in reflectance and standing crop biomass in three salt marsh communities. *Plant Physiology*, Vol. 58, pp. 696-699.

Ernst-Dottavio, C.L., R. Hoffer, R. Mroczynski, 1981. Spectral characteristics of wetland habitats. *Photogrammetric Engineering and Remote Sensing*, Vol. 47, No. 2, pp. 1695-1703.

Forbes, R.D., 1972. A Floral Description of the Fraser River Estuary and Boundary and Mud Bays, B.C., Fish and Wildlife Branch, B.C. Department of Recreation and Conservation.

Fraser River Estuary Management Program, 1990. Habitat Inventory and Classification of Fraser River Main Arm, Pitt River, Sturgeon Bank, Roberts Bank and Boundary Bay.

Gates, D. M., H. J. Keegan, John C. Schleter, V. R. Weidner, 1965. Spectral properties of plants. Applied Optics, Vol. 4, No. 1, pp. 11-20.

Gilmer, D.S., E.A. Work, J.E. Colwell, and D.L. Rebel, 1980. Enumeration of prairie wetlands with Landsat and aircraft data. *Photogrammetric Engineering and Remote Sensing*, Vol. 46, No. 5, pp. 631-634.

Gower, J., and G. Borstad, 1981. Use of the *in vivo* flourescence line at 685 nm for remote sensing of surface chlorophyll *a*. In: J.F.R. Gower (ed.) Oceanography From Space. Plenum Press, New York, pp. 329-338.

Gower, J., G. Borstad, C. Anger, H. Edel. 1992a. CCD-Based Imaging Spectroscopy for remote sensing: The FLI and CASI programs. Canadian Journal of Remote Sensing, Vol. 18, No. 4;

Gross, M.F., and V. Klemas, 1986. Remote sensing of five saltwater marshes in France. *International Journal of Remote Sensing*, Vol. 17, No. 5, pp. 657-664.

Hardisky, M.A., F.C. Daiber, C.T. Roman, and V. Klemas, 1984. Remote sensing of biomass and annual net aerial productivity of a salt marsh. *Remote Sensing of Environment*, Vol. 16, pp. 91-106.

Harron, J.W., J. Freemantle, A. Hollinger, and J. Miller, 1992. Methodologies and errors in the calibration of a Compact Airborne Spectrographic Imager. *Canadian Journal of Remote Sensing*, Vol. 18, No. 4, pp. 243-249.

Hoffer, Roger, 1978. Biological and Physical Considerations in Applying Computer Aid Analysis Techniques to Remote Sensor Data, in: Remote Sensing: The Quantitative Approach, ed. P.H. Swain and S. M. Davis, pp. 227-289.

Hoos, Lindsay, and G. Packman, 1974. The Fraser River Estuary: Status of Environmental Knowledge to 1974. Special Estuary Series No. 1, Environment Canada.

Horler, D.N., M. Docray and J. Barber, 1983. The red edge of plant leaf reflectance. *International Journal of Remote Sensing,* Vol. 4, pp. 273-288.

Howland, W.G., 1980. Multispectral aerial photography for wetland vegetation mapping. *Photogrammetric Engineering and Remote Sensing,* Vol. 46, No. 1, pp. 87-99.

Hunter, R. A., 1983. Estuarine Habitat Mapping and Classification System Manual. Ministry of Environment Manual 3, Province of B.C..

Jensen, J.R., M.E. Hodgson, E.J. Christensen, H.E. Mackey, L.R. Tinney, and R.R. Sharitz, 1986. Remote sensing inland wetlands: A multispectral approach. Photogrammetric Engineering and Remote Sensing, Vol. 52, No. 1, pp. 87-100.

Kistrtiz, Ron, 1990. Habitat Inventory and Classification of Fraser River Main Arm, Pitt River, Sturgeon Bank, Roberts Bank, and Boundary Bay. Fraser River Estuary Management Program, New Westminister, B.C., 11 pp.

Lillesand, T., and R. Kiefer, 1987. Remote Sensing and Image Interpretation, 2 ed., Wiley, New York; 721 pp.

McDowell, D.Q. and M.R. Specht, 1974. Determination of spectral reflectance using aerial photographs. *Photogrammetric Engineering and Remote Sensing,* Vol. 40, pp. 559-568.

McLaren, K.A., 1972. A Vegetation Study of the Islands and Associated Marshes in the South Arm of the Fraser River, British Columbia, from the Deas Island Tunnel to Westham Island Foreshore. Fish and Wildlife Branch, British Columbia Department of Recreation and Conservation. 55p.

Moody, A.I. 1978. Growth and distribution of the vegetation of a southern Fraser delta marsh. University of British Columbia, Department of Botany, M.Sc. thesis.

Penuelas, J., J.A. Gamon, K. Griffin, and C. Field, 1993. Assessing community type, plant biomass, pigment composition, and photosynthetic

efficiency of aquatic vegetation from spectral reflectance, *Remote Sensing of Environment,* Vol. 46, pp. 110-115.

Reimhold, R. J., J.L. Gallagher, D.E. Thompson, 1973. Remote sensing of tidal marsh, *Photogrammetric Engineering and Remote Sensing,* Vol.?, pp. 477-488.

Roberts, A.R., and J. P. McDonald, 1992. Digital classification of salmon spawning habitat: An evaluation of airborne multispectral video imagery. Proceedings of the 15th Canadian Symposium on Remote Sensing. Ontario Center for remote sensing, John K. Hornsby, ed.

Savastano, Kenneth J., K H. Faller, R L. Iverson, 1984. Estimating vegetation coverage in St. Joseph Bay, Florida with an airborne multispectral scanner. *Photogrammetric Engineering and Remote Sensing,* Vol. 50, No. 8, pp. 1159-1170.

Slater, Philip, 1989. Systems, radiometric calibration, and atmospheric correction in remote sensing. *International Congress on Optical Science and Engineering,* Paris, France, 31 *pp.*

Story, Michael, and R.G. Congalton, 1986. Accuracy assessment: A user's perspective. *Photogrammetric Engineering and Remote Sensing,* Vol. 52, No. 3, pp. 397-399.

Tamburi, A., and S. Hays, 1978. An Introduction to River Mechanics and the Lower Fraser River. Department of Public Works of Canada, Pacific Region, Vancouver, B.C.; 71 pp.

Tucker, C.J., and L.E. Miller, 1977. Soil spectra contribution to grass canopy reflectance. Photogrammetric Engineering and Remote Sensing, Vol. 43, No. 6, pp. 721-726.

Tucker, C.J., 1979. Red and photographic infrared linear combinations for monitoring vegetation. *Remote Sensing of Environment,* Vol. 8, pp. 127-150.

Ward, P., K. Moore, and R. Kistritz. 1992. Wetlands of the Fraser Lowland, 1989: An Inventory. Technical Report Series No.146, Canadian Wildlife Service; 216 pp.

Weinmann, F. and M. Boule, 1984. <u>Wetland Plants of the Pacific Northwest.</u> U.S. Army Corps of Engineers, Seattle District; 85 pp.

Zacharias, Mark, O. Niemann, and G. Borstad, 1992. An assessment and classification of a multispectral bandset for the remote sensing of intertidal seaweeds. *Canadian Journal of Remote Sensing*, Vol. 18, No. 4 pp. 263-274.

## APPENDIX A: TERMS

**Brackish water**- Water which contains between 0.5 and 18 ppt. dissolved inorganic salts, also referred to as estuarine water.

**Estuarine marsh**- Marsh subjected to tidal mixing of freshwater and sea water. Ninety-two percent of marshes in the Fraser delta are classified as estuarine marsh, characterized by growth of cattail, sedge and bulrush. The salt wedge extends as far upriver as Annacis Island during spring low flow.

**Forb**- Broad leafed herb or herbaceous plant, other than a grass.

**Forest**- An area within which tree life forms 10 meters or taller comprise the dominant cover. May be found on fluvial, marine, till, and bedrock/colluvial derived sites.

**Freshwater**- Water which contains less than 0.5 ppt dissolved inorganic salts.

**Organic material**- Surface material comprised of greater than 30 % organic material by weight.

**Jetty**- Man made structure which includes training walls, weirs, and breakwaters extending into the water. Jetties are found within a channel or constructed perpendicular to the shoreline for the purpose of channeling and directing stream or tidal flows, preventing channel shoaling by littoral materials or retarding shoreline erosion by trapping littoral drift.

**Marine**- Water which contains greater than 18 ppt inorganic salts.

**Marsh**- A generally low gradient area which supports significant (15%) non woody vascular vegetation for at least part of the year and is characterized by a surface accumulation of organic material deposited in water. A marsh can be freshwater, estuarine, or salt marsh, dependent on the water supply.

**Integration time**- Time required by imaging instrument to sample and record radiance values in each band.

**Low Marsh**- Intertidal marsh exposed at low tides and covered at most moderate and all high tides. Little or no soil development, low species diversity, hydrophilic and often halophytic pioneer species and often discontinuous cover. Dominated by sedges, glasswort, sea milkwort, sea plantain.

**Micrometer ($\mu$m)**- Unit of measurement; $1 \times 10^{-6}$ meters. .550 $\mu$m is equal to 550 nm.

**Nanometer (nm)-** Unit of measurement; $1 \times 10^{-9}$ meters. The sensitivity range of the Compact Airborne Spectrographic Imager is 430 to 900 nm. The peak of wavelength of incoming solar radiation is also 540 nm, which is in green region of the visible spectrum.

**Shrub-** A low (> 2 meters in height) woody bush which usually has several stems. Typical shrub species are willow, Pacific crab apple, blackberry, roses, red alder, and are defined as being less than six feet tall. Shrubs prefer mineral soils which are periodically saturated but rarely inundated.

**Radiance-** The radiant flux per unit solid angle per unit of a projected area of a surface expressed in microwatts per square centimeter per steradian per nanometer ($mW\ cm^{-2}\ sr\ nm$).

**Reflectance-** Amount of energy incident on earth's surface that is neither absorbed or transmitted. Reflectance is often expressed as a percentage of the total incident energy to reduce environment variability and sensor dependent variables.

**Spectral response-** Behavior of incident energy on a surface. Energy is either reflected, absorbed or transmitted. In visible and near infrared remote sensing, reflectance is the measured variable.

**Steradian (sr)** - Unit of solid angle on a sphere, where four steradians will account for complete coverage of the surface of a sphere. Radiance is expressed as watts per square meter per steradian.

**Tide channel-** Channel resulting from and dominated by tidal processes. Tidal channels flush and drain the intertidal portion of deltas or marshes and are often characterized by silty organic bed materials and steep banks. Emergent and submergent vegetation is often present, as well as algal mats.

**Training Area-** An area in an image representative of a known land cover types, substrate or vegetation species. The pixels in the training area contain radiance information from each band of data collected, and the radiance values are used to define the spectral response of the area and find other areas in an image with similar spectral response.

*Sources: Lillesand and Kiefer (1987), Colwell (1974), Hoffer (1978). All marsh definitions from Hunter (1983).*

## APPENDIX B: CASI OVERVIEW

The Compact Airborne Spectrographic Imager is an airborne digital imaging spectrometer developed in Canada and initially designed for space orbit. A multispectral imager collects surface radiance values in specific and narrow spectral bands, while aerial photographs record radiance as gradations of photographic tone. Airborne multispectral imagery has a higher spectral and spatial resolution than satellite imagery, and the instrument is accessible for calibration for a specific application. The CASI instrument can be used for other estuarine monitoring projects, like dinoflagellate blooms, water quality, and pollution plumes. Much initial research with CASI imagery centered on the land water interface, including the detection of chlorophyll a to estimate phytoplankton pigment concentrations (Gower and Borstad 1981). Day (1989) has documented young salmon following zooplankton blooms, which follow just out of phase with a phytoplankton peak. CASI has also been used in the location of herring schools (Borstad and Hill 1989), surface oils spills and industrial effluent (Borstad 1992), and intertidal vegetation such as eel grass beds and intertidal seaweed (Zacharias et al. 1992, Anger et al. 1990).

Radiance from the earth's surface is viewed by the instrument optics, split by a diffraction grating and measured on a silicon based charged coupled device (CCD) sensitive to the wavelength range of 418 to 926 nm. The spectrometer provides a high resolution (minimum bandwidth is 2.9 nm) spectrum for each picture element (pixel). Spatial resolution varies with integration time, speed and altitude of aircraft, number of bands and bandwidth. Frame rate and ground speed determines along-track pixel size.

Altitude of aircraft determines cross-track pixel size. The instantaneous field of view (IFOV) is 1.2 milliradians, the field of view (FOV) is 35 km. Because the platform is airborne rather than spaceborne, the distance to the target is minimized and thus atmospheric scattering and absorption are reduced.

In spatial mode the swath is divided into 512 pixels and up to 15 spectral bands can be recorded for each pixel. Integration time in spatial mode is approximately 50 msec. (Gower et al. 1992a).

Harron et al. (1992) demonstrate the error of absolute spectral response to be 1.9%, which can be dominated by systematic errors. Radiometric error associated with instrument operation is 2 to 4 percent, although Anger et al. (1990) report a radiometric calibration accuracy of 5% and a wavelength calibration of +- 1 nm.